A MICROFLUIDIC METHOD FOR DETERMINING THE MOLECULAR WEIGHT OF POLYMERS OF UNKNOWN CONCENTRATIONS

A Thesis
Presented to
The Academic Faculty

by

Melissa Li

In Partial Fulfillment
of the Requirements for the Degree
Master of Science in the
School of Biomedical Engineering

Georgia Institute of Technology
2008

A MICROFLUIDIC METHOD FOR DETERMINING THE MOLECULAR WEIGHT OF POLYMERS OF UNKNOWN CONCENTRATIONS

Approved by:

Dr. Hang Lu, Advisor
School of Chemical and Biomolecular Engineering
Georgia Institute of Technology

Dr. Rachel Chen, Advisor
School of Chemical and Biomolecular Engineering
Georgia Institute of Technology

Dr. Johnna Temenoff
Department of Biomedical Engineering
Georgia Institute of Technology

Dr. Yonathan Thio
School of Polymer Textile and Fiber Engineering
Georgia Institute of Technology

Date Approved: August 20, 2008

ACKNOWLEDGEMENTS

This work was made possible by generous contributions from a number of people. Thanks to Alison Hirsch, Gina Cremona, for their assistances with patterning wafer molds, Matthew Crane and Ivan Caceres for help with Matlab, and to Taymour Hammoudi for assistance with the PEG-DA surface treatment experiments.

Thanks to the members of the Chen lab, especially Dr. Zichao Mao and Dr. Hyun-Dong Shin for providing the samples of culture HA analyzed in this work; to Jay Sy and the Murthy lab for sample dialysis and lyophilization; to Dr. Johnna Temenoff's lab for the contribution of some reagents; to Ryan Kincer and the Beckham group for the use of the Ubbelohde viscometer; and to Genggeng Qi and the Jones group for GPC processing and analysis.

Thanks to Dr. Yonathan Thio and Jeff Stirman for helpful comments and advice with this work. Finally, thanks to all of the Lu group members for their guidance, support, and teaching.

TABLE OF CONTENTS

LIST OF TABLES

LIST OF FIGURES

LIST OF SYMBOLS AND ABBREVIATIONS

η_{sp}	Specific Viscosity (unit-less)
η_{rel}	Relative Viscosity (unit-less)
τ	Shear Stress (N/m^2)
$\overline{M}_w$	Weight averaged molecular weight (Da)
$\overline{M}_n$	Number averaged molecular weight (Da)
$\overline{M}_v$	Viscosity averaged molecular weight (Da)
K	Mark-Houwink coefficient ($\frac{cm^3}{g}(\frac{g}{mol})^{-a}$)
a	Mark-Houwink exponent
$[\eta]$	Intrinsic Viscosity (dLg^{-1})
d_h	Hydraulic Diameter (m)
D_{AB}	Diffusion constant of species A into B (cm^2/s or m^2/s)
ρ	Fluid density (kg/m)
M	Molecular Weight (Da)
t	time (seconds)
PEO	Poly-ethylene Oxide
HA	Hyaluronic Acid
PDMS	Poly-dimethyl Siloxane

SUMMARY

Molecular weight and concentration are two most important characteristics of polymers synthesized through chemical or microbial processes. However, current methods for characterizing polymer molecular weight such as Multi-Angle Laser Light Scattering (MALLS) or Gel Permeation Chromatography (GPC) require long processing and analysis times, expensive equipment, high sample concentrations, and high sample volumes. These limitations prevent dynamic time-point studies of changes in molecular weight, which would be very useful for monitoring synthesis progress in microbes or in chemical synthesis.

In this thesis, we designed, fabricated, and tested a rapid, low cost, high throughput, modular microfluidic system for determining polymer molecular weight in samples of unknown concentrations. The system evaluates molecular weight by evaluating the viscous behavior of polymers in various solvent conditions to their molecular weights. It consists of two modules for measuring fluid viscosity, and for controlling solvent conditions.

Results of this study will show that this system is able to evaluate the differences in polymer viscosity for varying molecular weights and solvent conditions. For the solvent control module, we show that salt concentrations in small titers of polymer solutions can be rapidly added or subtracted and evaluated compared with current

methods. Next, we show the efficacy of the viscosity module at rapidly assessing fluid viscosity over a wide range of molecular weights. Finally, we show the effects of solvent changes on molecular weight viscosity, and thus the efficacy of the system in determining molecular weight from fluid viscosity. This system is applied to the evaluation of both the biologically produced polymer Hyaluronic Acid (HA) and the synthetically produced polymer Poly-ethylene Oxide (PEO).

In conclusion, we present proof of concept of a modular microfluidic system for evaluating polymeric molecular weights without prior knowledge of concentration. Future work and applications for such a system would be its application to the research of dynamic synthesis of biopolymers and for industrial chemical syntheses.

CHAPTER 1

INTRODUCTION

Polymers are a class of commercially important, long-chain molecules. One of the most common ways in which polymers are evaluated by is molecular weight. Molecular weight is a valuable metric because it indicates the length of the polymer chain, which in turn determines its chemical and mechanical behavior. Thus, the recent developments of polymer production using engineered microbes as well as advances in polymer synthesis have made molecular weight characterization methods extremely important. High-throughput molecular weight characterization would allow studies examining how the conditions under which a polymer is produced can affect the product over parameters such as time, substrate concentrations, catalyst addition, etc.

However, molecular weight is a complex property that is not easily determined using traditional methods, especially for the dilute and uncharacterized concentrations of polymer obtained from synthesis or microbial fermentation. Such traditional molecular weight characterization methods are limited by high costs, low throughput, and the need to know the concentration of sample in the solution. Costs are high due to the use of large, complex, and highly automated hardware. Throughput is low due to long sample preparation and processing times (hour scale), high sample concentrations (milligrams/milliliter scale), and high sample volumes (milliliter scale). Although these concentrations and volumes may seem small relative to current technologies, they are significant when dealing with quantities relative to metabolically engineered microbial

fermentation products, when product is produced on the microgram/milliliter scale over a period of hours.

This work addresses these issues by presenting a low cost, high throughput method for determining the molecular weight of polymeric samples of unknown concentration by measuring their viscosity in varying solvent conditions. This chapter introduces important themes and concepts, which will be further discussed in this work. Specifically, it will provide an overview to polymer molecules and their characterization, microfluidics, and metabolic engineering. It will also show the ways in which the simultaneous use of all of these different fields can provide significant advantages and opportunities when compared with current methods.

1.1 Polymers

Polymers are long-chain molecules composed of repeating structural monomer units and can be manufactured through either synthetic or biological means. The number of these monomer units contained within a polymer determines its overall molecular weight, which can vary from the hundreds to the millions of Daltons. The configuration of the monomer units can vary as well from linear to branched chains, or cross-linked networks of chains [1]. One way in which polymers may be categorized is by their origins: biologically derived "biopolymers", or synthetic polymers engineered from monomers through directed chemical reactions.

A great number of biologically produced polymers exist in the natural world, such as the well-known celluloses and rubbers produced by plants [3]. Recently, polymers produced by animal cells from humans to microbes have also come to prominence.

Examples include molecules such as hyaluronan, curdlan, and pullulan as well as those the well-known DNA and RNA. While the functions of the latter two are well-known, the former are also widely used in industry as food additives and as biocompatible coatings [4]. Another benefit of biopolymers is that they are environmentally friendly for manufacturing and disposal since most can be digested enzymatically.

Within the last century synthetic polymers have had the most impact in industrial areas such as films, clothing fibers, plastics, and glues. Recently, these synthetics have been used for biomedical applications for hard and soft tissue implants, drug coatings, and as scaffolds for tissue engineering [5].

Both synthetically and biologically derived polymers must undergo molecular weight characterization. Biopolymers are especially important to characterize due to the complex, time dependent polymerization reactions by which they are produced. Synthetic polymerization products of high molecular weight are also subject to quality control molecular weight characterizations [1, 3, 6].

Given this wide range of applications, the importance of both manufacturing and characterizing polymers is apparent. As noted earlier, polymers can be manufactured synthetically or biologically. However, laboratory synthesis of polymers can be expensive, time consuming, and difficult. One solution to these issues is the use of microbial polymer synthesis using metabolic engineering. Metabolic engineering is the genetic modification of microbes to optimize their production of specific complex molecules. Using these methods, it is possible to produce engineered long-chain polymers *in-vivo,* which have proven difficult to synthesize.

Characterization is a necessary process for all polymers—whether synthetic or naturally derived. Generally the most important characteristic to determine is molecular weight, a characteristic which varies based on the method used. However, many commonly used methods such as GPC and macroscale capillary viscometry for molecular weight characterization are low throughput and require extensive manual sample preparation. In contrast, this method seeks to establish a high throughput method with little manual sample preparation.

1.2 Metabolic Engineering

The ability to produce polymers from a living organism presents a number of advantages over chemical synthesis. First, biopolymers often have complex structures which are difficult to replicate synthetically. Second, biologically produced polymers do not require the use of dangerous or expensive chemicals required for synthesis such as boron fluoride for the synthesis of PEO. Third, chemical synthesis often requires the use of special chemical, temperature or pressure conditions that are difficult to replicate outside of a dedicated production plant. Thus, production of polymers from microbial hosts is a desirable solution. Metabolic engineering is the controlled construction or re-arrangement of a host cell's metabolic pathways. These alterations cause the host to produce specific substances when grown under controlled conditions, transforming the host into a "microbial cell factory" [7]. Since its recent inception, the field has undergone impressive growth and shown great promise for the biomedical community. In recent years, metabolic engineering has produced materials for applications from surgical coatings and synovial fluid replacements to low-cost malarial vaccines [8]. The

production of such complex molecules using whole cells is very attractive due to excellent sustainability (due to low maintenance costs) and good system robustness [8].

Characterization of these complex molecules is essential for establishing and maintaining these microbial factories. Often cellular production is a dynamic process, thus continuous monitoring of microbial cultures is desirable. For instance, the molecular weight of the biopolymer hyaluronan has been observed to undergo considerable fluctuations in molecular weight and polymer polydispersity over varying culture times[9]. Molecular weight is an important property of many biopolymers because it determines structure and function. For example, samples of low molecular weight HA have been shown to be immunogenic, while samples of high molecular weight have been shown to have strong anti-immunogenic effects [4, 10]. Currently, however, purifying and determining the concentration of biologically produced molecules is a time-consuming and tedious process. First, the crude product must be repeatedly washed. Next it is filtered using dialysis and membrane filters. Finally the purified product is weighed. This step is often problematic since the balance must be large enough to be recognized by the scale. Since biopolymers such as HA are produced on the scale of micrograms per milliliter over the timescale of days, this requires large culture volumes and long wait times. Also, purification is often an inefficient process, resulting in significant product loss and low sensitivity.

Thus Metabolic Engineering is an important emerging field which would benefit greatly from a biopolymer characterization method which requires only small, dilute, and undetermined quantities of sample which can be examined in a high-throughput manner.

Although there is no current method which can address these issues well, one possible solution for creating such a method is the use of microfluidics.

1.3 Microfluidics

Microfluidics is a field which deals with behavior and control of small amounts of fluid on the micro- to femto- liter scale. Since it deals with such small amounts of fluid, the advantages of a microfluidics approach includes small sample small sample sizes, smaller timescales due to smaller transport lengths, high throughput, parallel processing ability, and lower costs [11, 12]. Thus far, microfluidics has proven effective in a number of routine laboratory activities such as flow cytometry [13], polymerase chain reaction (PCR) [14], and cell lysis.

Microfluidic methods provide a valuable tool set for characterizing both synthetically and biologically produced polymers by virtue of low volume, rapid, and high throughput sample processing that would allow monitoring of changes in molecular weight over time for production engineering and quality control. Small sample volumes would be minimally invasive to the synthetic or biological production apparatuses, and rapid analyses would allow a better understanding of the production mechanism and a subsequent opportunity to optimize the system.

Thus the field of microfluidics provides a valuable set of tools for the study of polymers due to advantages of low sample volumes, rapid testing, high throughput, and low cost.

Both biologically and synthetically derived polymers have a multitude of applications, thus methods for their production and characterization are important areas

of study. This work attempts to address this issue using the low-volume, high throughput advantages of microfluidics for sample analysis of complex polymers. These advantages are especially important for the optimization of processes involving the in-vivo creation of polymers through the field of metabolic engineering.

CHAPTER 2

BACKGROUND

This chapter will discuss the theoretical background surrounding this project. First it will address the physical nature and structure of biological and synthetic polymers, with special attention to two specific examples. Next it will discuss the importance of the viscosity of polymer solutions in determining the relationship between polymeric molecular weight and its solvent. Finally, it will discuss current methods for measuring solution viscosity and how they provided comparisons and contributions to the development of this work.

2.1 Polymers

Polymers are an integral part of biomaterials and biomedical applications. For this work two model polymers, one of biological and the other of synthetic origin, have been chosen for study. Polyethylene oxide (PEO) serves as the model synthetic polymer and the model biopolymer is Hyaluronic Acid (HA). Synthetic polymers are desirable to study for their generally low polydispersity and high levels of purity relative to biopolymers. In contrast, the study of biopolymers can provide insights into the applications of this method to the field of metabolic engineering.

The following section will further discuss reasons why these two particular polymers have been chosen for study and specifics of their structures and functions. It will also address the causes and possible solution for three central issues in characterizing

the formation of biological or synthetic polymers: small, dilute unknown concentrations of polymer and time sensitive changes.

2.1.1 Model Biological Polymer: Hyaluronic Acid

The biopolymer Hyaluronic Acid (HA) has been specifically chosen for its structural properties and its in-vivo method of synthesis.

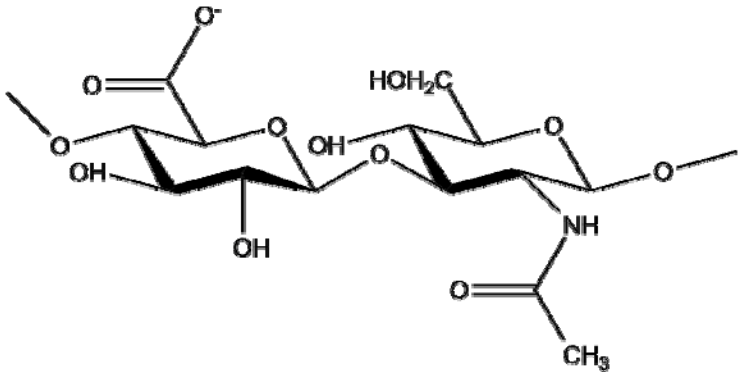

Figure 2-1: *The HA monomer*

Although there are a number of commercially important high molecular weight biopolymers such dextran, pullulan, and cellulose, hyaluronic acid (HA) has a unique set of biomedical properties and is known to reach some of the highest molecular weights (~0.5 to 4MDa) [4]. This high molecular weight has been shown to determines HA's function: high molecular weight HA (>10^6) is extremely viscoelastic and anti-immunogenic, while low molecular weight HA (<10^5 Da) is less viscoelastic and very immunogenic [4]. Some of its unique biomedical advantages are listed below:

Category	Specific Application
Surgery	Non-immunogenic coating for ophthalmic surgical tools [2]
Cosmetics	Active agent in many new skin-care lines to enhance skin elasticity [2]
Pharmaceuticals	Non-immunogenic, biodegradable coating for drug delivery [2, 15, 16]

Dermatology	Subcutaneous wound healing [2]
Public Health	Assessment of microbial pathogenicity
Medical	Treatment of osteoarthritis by injection into synovial fluid of knees and other joints [2]
Cosmetic Surgery	Injectable cosmetic skin filler marketed as a collagen alternative [2]

Table 2-1: *Commercial applications of Hyaluronic Acid (HA)*

HA is secreted from cells as an exopolysaccharide—a thick polymer layer which forms a cell's extracellular matrix. In the past, HA has been primarily derived from complex animal sources such as rooster combs, bovine vitreous humor, and human umbilical cord. However, these sources are flawed by low yields, laborious extractions, large amounts of contaminants, and high concentrations of inflammatory factors relative to microbial sources [17]. Another source of HA found in nature is on the extracellular coats of pathogenic microbes such as Pasteurella multocida and Streptococcus pyogenes [9]which use the polymer to evade detection by the immune system [18].

Recently, however, laboratory safe microbes such as Lactococcus lactis, Agrobacterium, and Escherichia coli have been used as hosts for the production of high molecular weight HA using genes derived from these pathogens. A study of the molecular weights of culture products by Yu *et al.* from one such recombinant strain yielded HA with molecular weights of 0.38 and 1.7 MDa secreted into culture broth at time points of 24 and 72 hours in concentrations of 154.8μg/mL and 203.5 μg/mL, respectively [9].

Two important observations can be made from Yu's experiments. First, there exists a large, *time-dependent* increase in the average molecular weight and the range of molecular weights in solution. Second, polymer concentration increases non-linearly at

different culturing time points and under various culturing conditions, but remains within the dilute (<350mg/L) regime.

Although there is a clear need for time point studies within this field, current methods are insufficient to address it. The most pressing issue is that the analysis of such time point products requires concentrated titers of analyte, which can only be obtained from large amounts of the dilute amounts contained in culture broth. The dilute nature of these titers, and the large overall volumes, requires that samples be dialyzed, lyophilized, filtered, and re-suspended over the course of days.

For these two reasons, the ability to identify molecular weight in a rapid, high throughput manner over a number of different culturing times and conditions could provide a great deal of information on understanding and controlling the production of HA in microbes.

Although HA is of primary interest to us, its high costs make it desirable to first test the method proposed in this paper on a polymer which is of a similar structure, but lower cost and easily obtained. For this purpose, we have chosen the synthetic polymer Poly-Ethylene Oxide to test our method.

2.1.2 Model Synthetic Polymer: Poly-Ethylene Oxide

Polyethylene oxide (PEO) is a synthetic polymer chosen for its molecular structure, its existing body of knowledge, commercial value, and current characterization methods. The molecule itself is composed of two polar hydroxyl groups surrounding a monomer of two hydrophobic ethylene groups joined by hydrophilic oxygen [19].

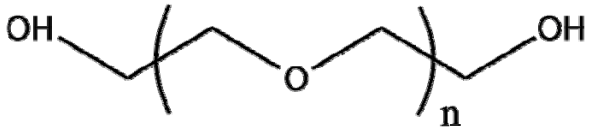

Figure 2-2: *The PEO monomer.*

This monomeric unit is arranged into a linear chain. This lack of branching accentuates its conformational effects in solution, making it an excellent model for this work. PEO is also an excellent model for this work since its high molecular weight samples (~1-8MDa) are typically characterized using viscosity-based metrics such as those described in this work [19]. This feature makes our method of immediate use to current and commonly employed characterization methods for this polymer. Finally, the effect of salts on molecular conformation and solution viscosity of PEO has been noted and characterized by previous work [19] and is used in later sections for predictions of molecular conformational changes.

PEO is used for a variety of medical and industrial purposes [3] such as those listed by the table below:

Category	**Specific Application**
Paper	Thickener for aqueous suspensions of pulp and paper fibers[20]
Textile	Textile warp sizing agent, moisture absorber for acrylic fibers, binder/sizing agent for glass fiber [14]
Paint/Pigments	Thickener for water based paints, pigment dispersant, dispersant of paint for fluorescent lamp [14]
Ceramics	Effective flocculent for finely dispersed silica, clay, and coal fine particles in water [14]
Agriculture	Soil reformer and retention aid[20]
Agriculture	Spreading agents in agricultural sprays of seeds and chemicals[20]
Electronics	Cleaner of electric parts[20]
Printing Ink	Protective colloids for printing ink[20]
Copy machines	Additives in developing agents in copying machines[20]
Cement	Thickener for cement slurry[20]
Coating	Hydrophilic coating to increase water pressure in firehoses[19, 20]
Lubricant	Mold release agent and major component of personal lubricants [19, 20]
Biomedical	Bio-inert drug coating and wound dressing [19, 20]

Table 2-2: *Applications of PEO*

PEO is also an excellent model polymer because of the methods typically used for its molecular characterization. High molecular weight PEO, such as that used in this work, is most often evaluated by viscosity [19, 21], which makes the proposed method a commercially significant procedure.

PEO is also significant to the medical industry. It forms an excellent drug coating and lubricant due to its wide range of water solubility and aqueous swelling. When conjugated with various chemicals, PEG can increase drug half life, decrease immunogenicity, and prevent antigenic binding. These effects have been theorized to be due to PEG's large size in solution, which sterically inhibits other molecules from accessing the targets to whom it adheres [22]. Other advantages of this polymer are that it is ingestible and non-toxic.

PEO is synthesized through anionic polymerization attack on an ethylene oxide ring. First a precise amount of initiator is added to the reactant mixture of ethylene oxide. Next, the reaction is left to run over a period of around 24 to 96 hours, depending on the molecular weight desired. The molecular weight of the products of this polymerization is highly dependent on the chemical composition of the catalyst and the amount present in the mixture [23-25]. Thus it is in our interest to develop a small volume, minimally invasive monitoring system which could examine the efficacy of a number of different catalyst conditions.

From the information presented in this section, it is clear that there are three central problems in determining the molecular weight of biologically and synthetically produced polymers:

1) Polymers are often produced in *unknown dilute concentrations*: All current molecular weight characterization methods require precise knowledge of molecular concentrations, making long sample preparations necessary.
2) *Limiting culture volumes*: Removing relatively large amounts of culture or synthesized polymer will disrupt growth patterns in microbial solutions or chemical interactions in reactors. Also since many molecular characterization methods require highly concentrated samples for analysis, they often require large amounts of culture for a much smaller analyte volume. Ideally, a molecular weight assay would require small volumes of dilute culture fluid.
3) *Time sensitivity*: Many metabolic engineering experiments track the concentration of target molecules. However, for molecules like HA, time sensitivity of molecular weight is also an issue, as discussed previously. A rapid method for molecular weight analysis would also be helpful for evaluating transient or unstable analytes.

Thus a rapid analysis method for molecular weight of culture samples of unknown concentration in small dilute amounts would be invaluable to evaluating polymer production in biological and industrial manufacturing processes.

2.2 Molecular Weight Metrics and Methods

The molecular weight, or more accurately the molecular mass, of a molecule is measured in the units of Daltons. It is closely associated with physical characteristics of a polymer such as its viscosity and shear behavior in solution, optical properties, and chemical reactivity. Methods for determining molecular weight include mass

spectroscopy, osmometry, viscometry, size exclusion chromatography, and by light scattering.

Ideally a group of polymers would all have the same molecular weight. However polymer chains often exist as a statistical spread of different molecular weights, a quality known as polydispersity. Thus one can describe the molecular weight of polymer samples in multiple ways [3].

The three most common of these are number average molecular weight (Mn), weight average molecular weight (M_w), and viscosity average molecular weight (M_w). For any molecular weight distribution, the three can be loosely related as $M_n<M_v<M_w$. This is more easily observable from experimental plotting of the three different measurements for a single polymer sample [3].

Type of Molecular Weight Determined	**Associated Method(s)**	**Advantages**	**Disadvantages**
Weight-averaged molecular weight (Mw) $\overline{M}_w = \frac{\sum N_i M_i^2}{\sum N_i M_i}$ **(2- 1)**	· Size exclusion chromatography (SEC) also known as Gel Permeation Chromatogrpahy (GPC) when organic solvent is used as the mobile phase carrier	· Wide molecular weight range · Sensitive · high resolution · measures poly-dispersity · Wide molecular weight range · Measures polydispersity	· Requires semi-dilute , known concentrations · Sample preparation · Slow · High cost equipment required
	· Matrix Assisted Laser Desorption/Ionization – Time of Flight (MALDI-TOF)	· measures poly-dispersity · Wide molecular weight range	· Requires known concentration · Sample preparation · Slow
	· Multi-angle light scattering (MALLS)	· measures poly-dispersity	· Requires known concentration · Sample preparation
Number-averaged molecular weight (Mn) $\overline{M}_n = \frac{\sum N_i M_i}{\sum N_i}$ **(2-2)**	· End-group titration,	· Low cost	· Requires known concentration · Molecule- specific effectiveness
	· Colligative properties: boiling point/freezing point alteration	· Low cost	· Requires known concentration · Low resolution · Large volume

	· osmometry	· Low cost	· Requires known concentration · limited effectiveness for high molecular weights
Viscosity-averaged molecular weight (Mv) $\overline{M}_v = K\left(\frac{\sum n_i M_i^{\,a}}{\sum n_i M_i}\right)$ **(2- 3)**	· Viscometry	· Low cost	· Requires known concentration · low accuracy for low molecular weights

Table 2-3: *Current methods for determining polymer molecular weight [26]*

Despite having a variety of choices for molecular weight characterization methods, the utility of many of these options is limited by high costs, low throughput, and the need for large sample volumes and long preparation times. Furthermore, they require previous knowledge on the precise concentration of sample being analyzed, which is often difficult to determine for small volume samples [1].

This work focuses on the use of viscometry to analyze molecular weight. This method was chosen due to low cost and ease of use—also characteristics which also make it an excellent candidate for miniaturization, high throughput, and thus for microfluidics. The following section will discuss and compare viscometric molecular weight analysis with other available methods.

2.2.1 Number-Averaged Molecular Weight

The number averaged molecular weight is the total polymer weight divided by the number of polymers. It is mathematically defined as:

$$\overline{M}_n = \frac{\sum N_i M_i}{\sum N_i} \qquad (2\text{-}2)$$

Methods for determining number averaged molecular weight must thus determine the number of molecules within a polymer sample. The most commonly used methods

which obtain a number-averaged molecular weight are end-group titration and osmometry [3, 27].

Of these methods, end-group titration is conceptually the most straightforward. However, its effectiveness is dependent on a number of factors. First, the polymer's end groups must be quantifiable through titration reactions or by NMR spectroscopy. Second, the number of end groups per molecule must be consistent and well known. Next, the concentration of reactive end-groups must be sufficiently large to mask other effects which may be caused by other reactive groups on the molecule. The final requirement is that the molar mass of each molecule is sufficiently below 10^4 Daltons to prevent steric blockage of end groups. Thus the method is limited to short-chain, sparsely branched and monodisperse molecules of synthetic origin such as short chain polyesters and polyamides [1, 3].

Osmometry compares the pressure of the solute molecules against one solvent vs. another solvent to obtain number of molecules. It is a number averaged method because the solvent-solute relationship is dependent on the number of solute vs. solvent molecules on either side of the membrane. Its requirements for measurement are less strict than end-group titration. It requires a dilute solution of a known number of solute and solvent moles. One advantage of this method is that it can be used to determine an absolute molecular weight, thus no calibration is required. However, the accuracy of this process is limited by the sensitivity of the osmotic pressure sensor, and is not regarded as accurate for polymers with molecular weight above 10^6 Daltons [1, 3].

Finally, boiling point and freezing point (also known as colligative properties) can be used to determine molecular weight through their alteration with the addition of

known concentrations of polymer. However, they are most commonly used with low molecular weight samples, are low resolution, and require large sample volumes for measurement [1, 3].

2.2.2 Weight-Averaged Molecular Weight

In contrast to number-average methods, weight-average molecular weight is calculated using the average molecular size instead of finding the total number of molecules. It is defined mathematically as:

$$\overline{M}_w = \frac{\sum N_i M_i^2}{\sum N_i M_i} \tag{2-1}$$

Light scattering measures molecular weight by quantifying the amount of elastic light scattering (Raleigh scattering) from each polymer molecule. The relationship between molecular weight and light scattering can be described as:

$$\Delta R_\theta = Kc\overline{M}_w \overline{P(\theta)_z} \tag{2-4}$$

where ΔR_θ is the change in Raleigh scattering at a particular interference angle θ, $\overline{P(\theta)_z}$ is the average particle scattering factor which accounts for the effects of measuring scattering from large solute molecules with a relatively small wavelength, K is the optical constant which relates the property differences between the polymer solutes and solvent molecules, and the concentration c of the polymer molecules in solution. The strength of this technique lies in its wide range of molecular weight determination, typically from about 10^4 to $5\text{x}10^6$ g mol^{-1} [1, 3].

Despite these advantages, these molecular weight methods are hampered by the need for extensive, time consuming sample preparation and analysis. They are also often prohibitively expensive for smaller laboratories, since light scattering requires a

collimated light source and a photomultiplier to detect scattered light, while chromatographic methods require the purchase of an expensive pumping unit along with expensive individual columns for running various species and solvents [1].

2.2.3 Viscosity-Averaged Molecular Weight

Viscosity averaged molecular weight is determined through measurements of the differences in the viscosity of solvent alone against a series of solutions of varying concentrations of polymer dissolved in solvent. Factors which determine viscosity include the concentration of polymer, the solvent-solute interaction, and the molecular weight of the polymer. Viscosity is an attractive characterization method because the necessary equipment is low-cost, the process is relatively rapid, and because viscometric methods are already a common standard for many chemical companies [1, 3, 4].

Gel electrophoresis is a method which has been most successfully applied to sections of the viscous biopolymer deoxyribonucleic acid (DNA), and has more recently been applied to the biopolymer HA [28]. In this method, a solid gel made of polyacrylamide or agarose is molded and suspended in buffer. Polymer samples are next loaded into the gel, and an electric DC voltage is applied. Depending on the size of the molecules, the charged particles will migrate towards the pole of opposite charge. Molecular weights are then found by comparing migration patterns with purified samples. However, its effectiveness depends on relatively high concentrations and innate molecular charge in order to detect the polymer within the gel. Thus the application of this method to low concentrations of polymers such as those present in culture fluids in metabolic engineering is not non-viable [1, 3, 4].

Viscosity averaged molecular weight can also be measured using capillary viscometry. Through this method, the viscosity-averaged molecular weight is defined by the Mark-Houwink equation:

$$[\eta] = K\overline{M}_v^{\,a} \tag{2-5}$$

In this equation, $[\eta]$ represents the polymer molecule's intrinsic viscosity—the volume of the polymer molecule in a given solvent [29-31]. The K and a terms are empirical constants which describe the effect of the solvent on the corresponding viscosity averaged molecular weight, $\overline{M}_v$.

Briefly, in this method fluid is flowed slowly in a very thin glass capillary and the speed that it takes the fluid to flow from one end of the tube to another measures the fluid viscosity. Using known concentrations, the viscosity is then extrapolated to zero to obtain $[\eta]$, and K and a are empirical constants. Advantages of this method are its low cost and relatively rapid time for sample preparation and analysis.

The disadvantages of the viscometric method for determining molecular weight are that it is hindered by need for large volumes of samples of known concentrations to derive $[\eta]$. This equation and methods for capillary viscometry will be discussed further in the following sections [31].

This section has discussed current methods for determining molecular weight and the resultant need for rapid, low cost, high throughput methods for analyzing polymers. It has briefly described methods currently used for determining molecular weight and their shortcomings. One hindrance common to all of these methods is the need to know the concentrations of polymer in the analyzed sample, while various other methods are

plagued by high costs, extensive sample treatment and analysis times, low throughput, and limiting sample volumes.

One method which is low cost and relatively rapid is capillary viscometry. Thus this method will be highlighted and discussed further for use in a method to characterize polymers of unknown concentration and unknown molecular weight.

2.3 Solution Viscometry

Bulk solution viscosity can be simply defined in mechanical terms as a fluid's resistance to shear stress (τ) in the y-direction, perpendicular to the direction of the fluid flow v and can be defined by the equation:

$$\tau = \eta \frac{dv}{dy} \tag{2-6}$$

Due to their exceptional size, the addition of polymers to small-molecule or aqueous solvents changes the viscosity, or the resistance to shear, of a solution significantly. For a single molecule, changes in viscosity are due to the molecules resistance to flow, and thus correlated with molecular weight and shape.

The method for measuring molecular weight using changes in viscosity is known as dilute polymer solution viscometry and is a commonly used technique due to its relatively low cost and fast preparation and runtime. A polymer solution can be classified as "dilute" when its concentration vs. viscosity can be described as a linear plot, while the concentration at which the plot diverges from linearity is known as the entanglement point.

Dilute polymer solutions are used for two primary reasons. First, even dilute polymer solutions have significantly different viscous behavior when suspended in

solvents composed of homogenous small molecules. Second, the low concentration of solute molecules prevents intermolecular interactions which might skew readings of viscosity.

2.3.1 Specific and Intrinsic Viscosity

In solution viscometry, the viscosity of a complete solution of solute and solvent is defined by η, while the viscosity of the polymer solutes relative to the solvent alone is η_{sp},the "specific viscosity". The viscosity of the solvent alone is η_0. The relationship between the three can be defined as:

$$\eta = (\eta_{sp} + 1)\eta_0 \tag{2-7}$$

This equation is also written using $\eta_{rel} = \frac{n}{n_0}$ and re-arranging the terms to produce the following:

$$\eta_{sp} = \eta_{rel} - 1 \tag{2- 8}$$

These viscous properties η_{sp} and η_{rel} both describe the bulk behavior of a solution, and are thus quantifiable through experiments. Using this information it is then possible to describe the average viscous behavior of each molecule in solution. This individual particle viscosity is known as intrinsic viscosity or the limiting viscosity and is denoted by $[\eta] \text{or} (\frac{\eta_{sp}}{c})_{c\to 0}$. Intrinsic viscosity can be considered a shape constant, or drag coefficient in macroscale terms.

Ideally, the viscosity of the entire solution is the product of the average intrinsic viscosity of each polymer solute and solvent molecule.

$$\eta_{sp} = [\eta]c$$

However this expression is only true for infinitely dilute polymer solutions, and never occurs in experimental conditions due to intermolecular interactions. Instead, it can be more accurately defined for experimental results using a virial expansion to account for concentration effects of a multiple-particle system[3]:

$$\eta_{sp} = k_0[\eta]c + k_1[\eta]c^2 + k_2[\eta]c^3 \ldots \quad (2\text{-}9)$$

where k_0, k_1, k_2, etc. are dimensionless empirical constants.

For dilute solutions, the c^n term becomes exponentially smaller, and allows the higher order terms to be disregarded. It was proven theoretically and experimentally by Huggins[29,28] that the general virial expansion could be accurately described by the truncated expression[29]:

$$\eta_{sp} = [\eta]c + 0.4[\eta]^2 c^2 \quad (2\text{-}10)$$

In this equation, the constant 0.4, known as the Huggins constant, describes "the size, shape, and cohesive properties of solvent molecules and solute sub-molecules, but not on the number of molecules" [32]. It has been experimentally verified to range from about 0.3 to 0.5 depending on polymer molecular weight [3, 4] (explicit values in literature were available for the two model polymers discussed in this work). Thus this expression can relate a measured bulk viscosity to an expression for individual molecular shape, the intrinsic viscosity.

2.3.2 Intrinsic Viscosity and Molecular Weight

With the determination of a polymer molecule's shape quantified by its intrinsic viscosity, it is necessary to correlate this shape with mass. In the same way that a tightly coiled rope sinks faster than a loosely wound rope, the relationship between intrinsic viscosity and mass depends on the conformation of the polymeric chain. This

relationship is evident in the exponential relationship in the Mark-Houwink equation (below). Since these chains have variable internal charges and backbone stiffness, a single polymer molecule can assume a variety of conformations. For example, when the backbone bonds of the polymer are rigid and intramolecular bonding is minimal, the polymer will spread out in solution in a rod-like conformation. The system parameter which generally dominates this relationship is the interaction between the solvent and solute particles.

A general expression for this interaction is the well-known Mark-Houwink equation (alluded to earlier in section 2.1.3):

$$[\eta] = K\overline{M}_v{}^a \tag{2-11}$$

Here K is an empirical constant and a has been shown to provide information on shape of the molecule in the solution. The constant a ranges in value from 0 to 2, with the smallest value corresponding to the maximally compacted spherical form and the largest value corresponding to the maximally extended or rod-like form[30]. Since K and a are specific to the chemical interactions of the each polymeric monomer with the solvent molecules, these constants should be uniquely defined for each solvent-polymer (of varying molecular weight) combination.

Previously, this equation has been discussed for its ability to determine the viscosity averaged molecular weight for a given $[\eta]$, K, and a in conventional capillary viscometry methods. However, this equation can also be used to describe the range of intrinsic viscosities for a single molecular weight for known K and a conditions. The latter technique will be discussed more in the following section.

2.3.3 Predicting Molecular Weight from Unknown Concentrations

From the previous sections of this thesis, equations have been defined for relating the bulk viscous of a dilute polymer solution to the shape of the molecule itself (the Huggins equation) and then for relating the shape of the molecule to its molecular mass (the Mark-Houwink equation) [29].

$$\eta_{sp} = [\eta]c + k'[\eta]^2 c^2 \tag{2-12}$$

However, these two equations cannot yet be combined since concentration and intrinsic viscosity are coupled values. Thus another relationship is needed. A second equation can be provided by the Mark Houwink equation which provides a relationship for intrinsic viscosity without the coupled concentration term.

$$[\eta] = K\overline{M}_v{}^a \tag{2-10}$$

$$\eta_{sp} = [K\overline{M}_v{}^a]c + k'[K\overline{M}_v{}^a]^2 c^2 \tag{2-13}$$

Now there are three known or experimentally determinable terms η_{sp}, a, K and three unknowns M_v, $[\eta]$, and c. However, the M and c terms are still coupled. Thus a third relationship is necessary. In this work, we used the relationship of two solvent conditions defined as 1 and 2, each with their own distinct sets designated a_1, a_2, K_1, K_2 for their respective solvent conditions 1 and 2). Solvent conditions can be monitored adjusted to the desired compositions through the combined use of diffusion-based mixing and electrical resistance measurements. A schematic of which equations are known and which are unknown is below:

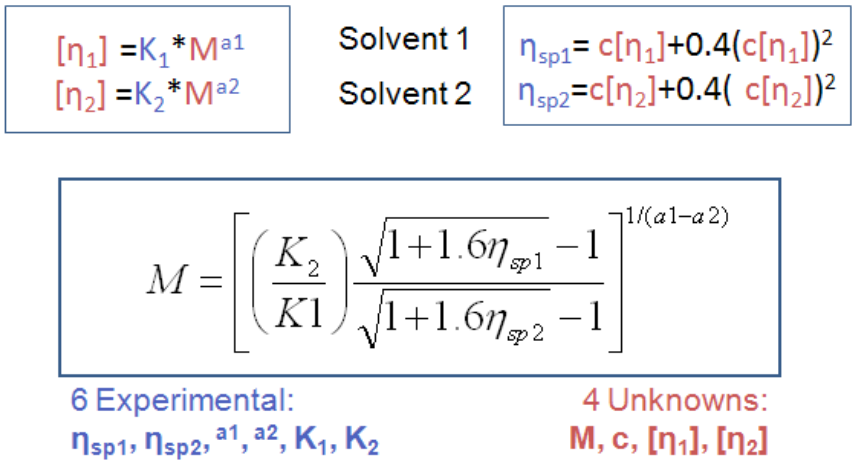

Figure 2-3: *Relating solvent conditions and viscosity to molecular weight. Experimentally determinable quantities indicated in blue and unknown in red*

Under these experimental conditions, the two equations can be combined to produce a relationship between pairs of measured specific viscosity for solutions of different solvent salt conditions (1 and 2) to solve for molecular weight.

$$M_v = \left[\left(\frac{K_2}{K_1} \right) \frac{\sqrt{1+4k'\eta_{sp1}} - 1}{\sqrt{1+4k'\eta_{sp2}} - 1} \right]^{1/(a1-a2)} \tag{2-14}$$

Thus for a single sample of a polymer solution of unknown concentration, one can measure the specific viscosity of the solution under two different solvent conditions to obtain a set of specific viscosity values. Combining these two specific viscosity values with previously determined *K* and *a* constants for the two solvent conditions, molecular weight can be estimated.

The plots in the following sections visualize the relationship between measured pairs of intrinsic viscosity points and the polymer molecular weight. By drawing a line

across the z-axis, one may obtain a line depicting predictions for pairs of specific viscosities η_{sp1} and η_{sp2} for each respective salt condition 1 and 2.

For this paper, the desired sensitivity range for this method on both the biopolymer HA and the synthetic polymer PEO is on the order of 1-2MDa, which is the current standard for commercially available samples of both polymers [33]. These predictions will be discussed in the following section. Although the predictions here show the range for 1-2MDa in molecular weight, the theoretical maximum sensitivity of this method is only limited by the precision of viscosity readings for each sample. The precision of the viscosity readings will be discussed in Chapter 5 and the actual experimental limits of the method's sensitivity will be discussed further in Chapter 6.

The next two sections will discuss predictions based solely on theoretical information. The relationship of this theoretical data with experimental values will be discussed in Chapters 5 and 6.

2.3.3.1 Poly-Ethylene Oxide Predictions

The prediction of the behavior of the model synthetic polymer, PEO, were made from obtaining literature values for constants, and then putting that equation into Predictions of the expected solution viscosities of PEO were made in the following manner. First, two specific solvent conditions were selected: (1) pure water, and (2) 0.45M K_2SO_4 salt in water. Next, a literature source[19] yielded specific values for the Mark-Houwink constants K_1, a_1 as well as K_2, a_2 constants relating the viscous averaged molecular weight to intrinsic viscosity measurements for the two aforementioned solvent conditions. Thus the equation (2-13) could be expressed more explicitly as:

$$M_v = \left[\left(\frac{0.0125}{0.130} \right) \frac{\sqrt{1+1.6\eta_{sp1}} - 1}{\sqrt{1+1.6\eta_{sp2}} - 1} \right]^{1/(0.76-0.5)}$$

$$M_v = \left[(0.0961) \frac{\sqrt{1+1.6\eta_{sp1}} - 1}{\sqrt{1+1.6\eta_{sp2}} - 1} \right]^{3.84} \quad \textbf{(2-15)}$$

From this equation, one can see for a pair of measured specific viscosities of different solvent conditions but of identical concentrations, a molecular weight can be derived. For a set of different concentrations, many pairs of specific viscosities may be obtained, thus increasing the stringency of the result for M_v. This now represent an equation with two input variables (η_{sp1}, η_{sp2}).

This figure shows the relationship between the specific viscosity in low salt concentrations (x axis), specific viscosity in high salt concentrations (y-axis) and Molecular Weight (z-axis). If one were to examine how x and y vary over a single value for Molecular Weight on the z-axis, it is clear that for that single z-value the specific viscosities in each salt condition describe a line. Each combination of x and y which forms a point on this line represents a unique pair of specific viscosities for these salt conditions at a certain concentration.

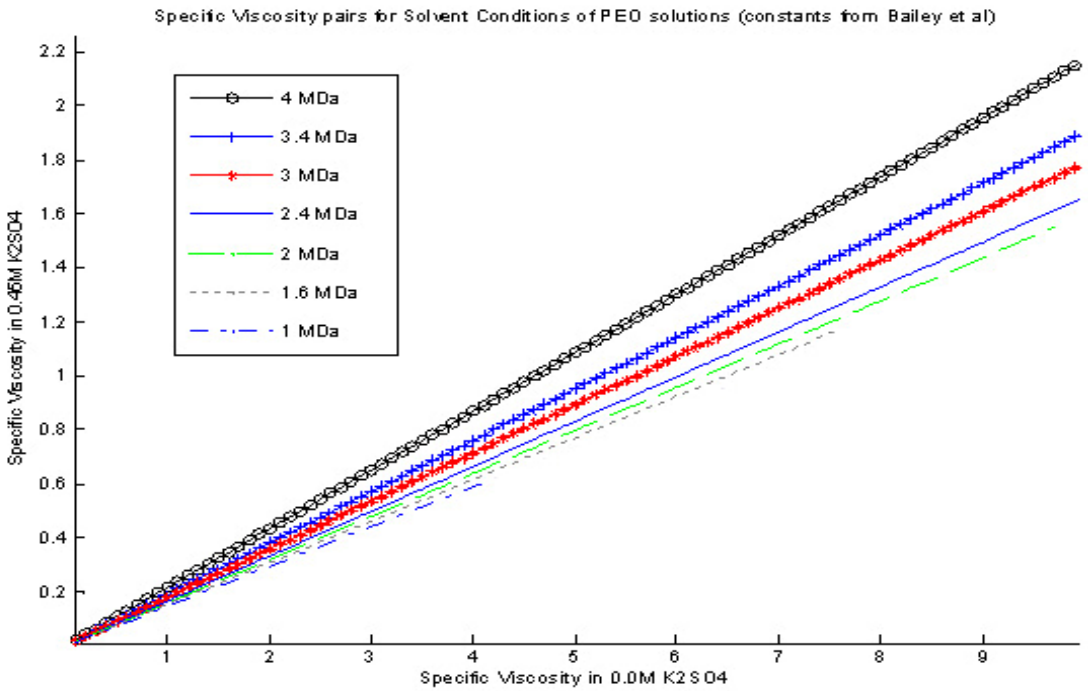

***Figure 2-4**: PEO specific solution viscosities in two solvent conditions for varying molecular weights*

Above is a plot where each line represents a different molecular weight, and each line represents the plotted specific viscosities of two solvent conditions for a polymer solution of an identical but unknown concentration. For instance, each red asterisk point has an x-coordinate which is its specific viscosity in 0M K_2SO_4, while its y-coordinate is its specific viscosity in 0.45M K_2SO_4. All of these points can be connected, forming a distinct linear series for that particular molecular weight of 3MDa. It is clear from this plot that as both molecular weights and concentrations increase, the viscous differences between samples increases as well. Practically, however, these predictions are only applicable to concentrations within the dilute regime, which ends at approximately 0.5% w/v. Using the *K* and *a* constants from literature provided for the conditions of 0M K_2SO_4 salt, the corresponding specific viscosity is 23 at the highest molecular weight of 4MDa, and the specific viscosity at the lowest molecular weight is 4. Thus the line for

the pairs of specific viscosity for different molecular weights terminate at different points, as can be seen in figure 2-5. Since the microscale capillary viscometer has been shown to be able to distinguish well between samples with differences of >5% of the total viscosity (see Chapter 5 for details), one can estimate using this chart the molecular weight resolution for several different molecular weights.

Thus we have shown in this section that molecular weight characterization of high molecular weight PEOs should be detectable with the application of the previously discussed method.

2.3.3.2 Hyaluronic Acid Predictions

Next, theoretical values for HA viscosity were calculated. HA constants for *K* and a values from the Mark-Houwink equation were taken from a number of literature sources to check for consistency for various sources. These constants were then used to examine pairs of viscosity for different solvent conditions for HA polymers of different molecular weight.

Literature figures for Hyaluronic Acid constants K and a			
Source	*a*	solvent	$K\ (\frac{cm^3}{g}(\frac{g}{mol})^a)$
Laurent 1960	0.78	0.3M NaCl	No data
Balazs 1965	0.8	0.3M NaCl	0.029
Cleland 1970	0.816	0.3M NaCl	No data
Shimada 1975	0.76	0.3M NaCl	No data
Bothner 1988	0.779	0.3M NaCl	No data
Fouissac 1992 (values used in this study)	0.78	0.3M NaCl	0.02859
	0.91	0.01M NaCl	0.01173
Gamini 1992	0.81	0.3M NaCl	No data
Yanaki 1994	0.829	0.3M NaCl	No data
Berriaud 1998	0.79	0.3M NaCl	No data
Takahashi 1999	0.79	0.3M NaCl	No data
Mendichi 2003	0.778	0.2M NaCl	No data

Hokputsa 2003	0.73	0.3M NaCl	No data
Armstrong 1997	0.841	0.1M NaCl	0.016
Cowman 2005	0.8	0.15-0.2M NaCl	0.029

Table 2-4: *HA K and a constants from literature*

These constants were then tested on commercially available HA to test the experimental adherence of this method to the predicted numbers. The explicit equation plotted can be expressed as:

$$M_v = \left[(2.4005) \frac{\sqrt{1+1.6\eta_{sp1}} - 1}{\sqrt{1+1.6\eta_{sp2}} - 1} \right]^{7.142857} \tag{2-16}$$

Next this study shows two sets of predictions: the first for the range of molecular weights given in the experimental results of Yu *et al.*, and the second for the range of molecular weights of hyaluronan that were available for experimentation.

For the first plot based on the data of Yu *et al.*, the range of molecular weights from 0.38 to 1.7 MDa was taken from the time-point experimental results of Yu *et al.* and the specific viscosity range highlighted in the charts shown was calculated for concentrations sufficiently below the entanglement point of the mean molecular weight and above the detection limit.

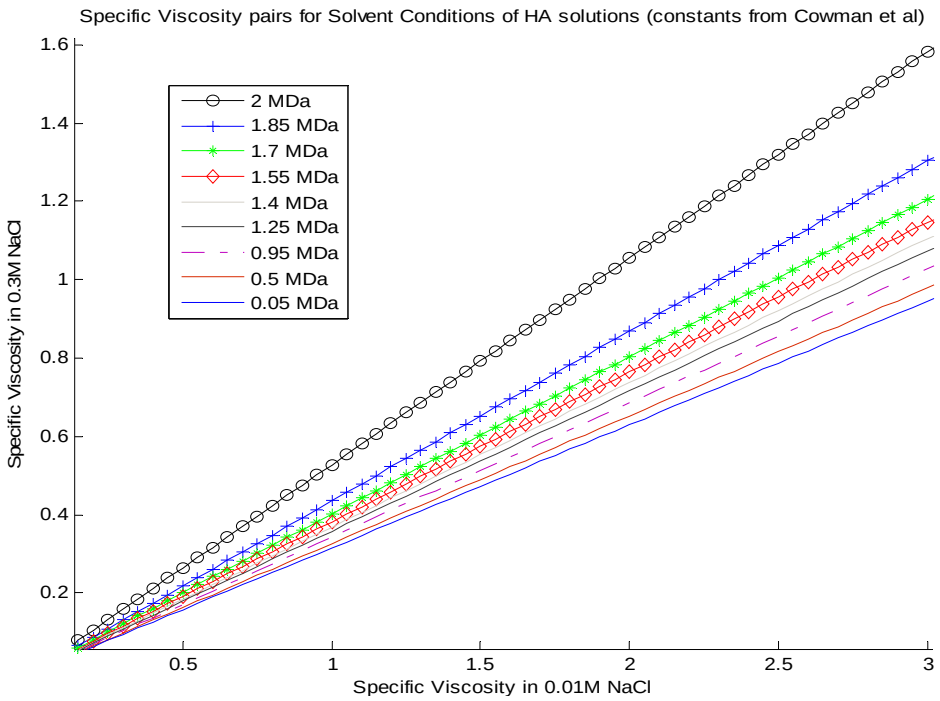

Figure 2- 5: *HA specific solution viscosities in two solvent conditions for varying molecular weights*

As with the predictive plot for the results of PEO, this plot predicts the differences in viscosity pairs for varying molecular weights to check if the predictions are within the detection limits of this system. From the plot above, it is clear that for the specific viscosity limit, there is a specific viscosity difference of about 0.7, an amount which falls well within the detection limit for this method, as will be further discussed in the Experimental Methods and Results sections.

This chapter has first shown the importance of molecular weight characterization for biological and synthetic polymers. It has further discussed the different definitions of molecular weight and the importance of these definitions to the form and applications of the polymer. It has also discussed the problems relevant to the design of a good characterization method, and the shortcomings of current methods.

With these design criteria in mind, this work has proposed a novel methodology for characterizing polymer molecular weight, and shown theoretical predictions of what our required detection limit needs to be in order to characterize the range of our interest.

CHAPTER 3

METHOD FOR DETERMINING MOLECULAR WEIGHT

This section will describe the specifics of the method proposed to determine molecular weight of a polymeric solution. First I will describe the process necessary to determine the parameters that are used in the calculation of molecular weight (theory discussed previously in Chapter 2). Second, I will describe use of the method to determine polymer solution viscosity. Components of this viscometer system can be divided into three modules: dialysis and sample pretreatment, viscometer, and post-processing.

3.1 Use of the System to Determine Molecular Weight

In Chapter 2 a theoretical treatment of the relationship between molecular weight, solvent conditions, and viscosity of dilute polymer solutions was discussed. In this chapter, the specific application of this equation to a methodology will be discussed.

The flowchart below describes the process that the molecular weight analysis system uses:

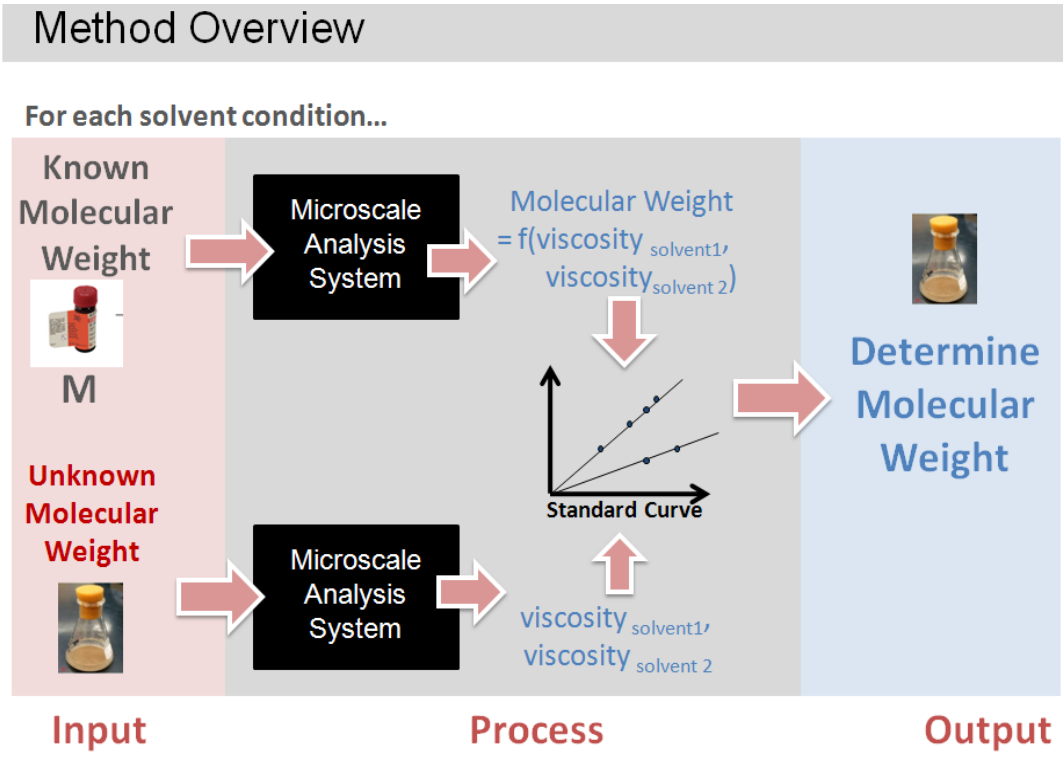

Figure 3-6: *Method of determining molecular weight of a polymer of unknown concentration.*

First, the polymer of interest is selected, and standards of characterized molecular weight and concentration are run through the viscometer system under two different solvent conditions to determine the constants a_1, a_2, K_1, K_2 for the Mark-Houwink equation (discussed previously in Chapter 2). These constants can be used for the final equation (2-13) determined previously:

$$M_v = \left[\left(\frac{K_2}{K_1} \right) \frac{\sqrt{1+4k'\eta_{sp1}} - 1}{\sqrt{1+4k'\eta_{sp2}} - 1} \right]^{1/(a1-a2)}$$

From this equation, one can construct a "standard curve" by plotting η_{sp2} as a function of η_{sp1} for certain values of M_v. This technique was shown previously in Chapter 2 when standard curves for PEO and HA predictions were constructed.

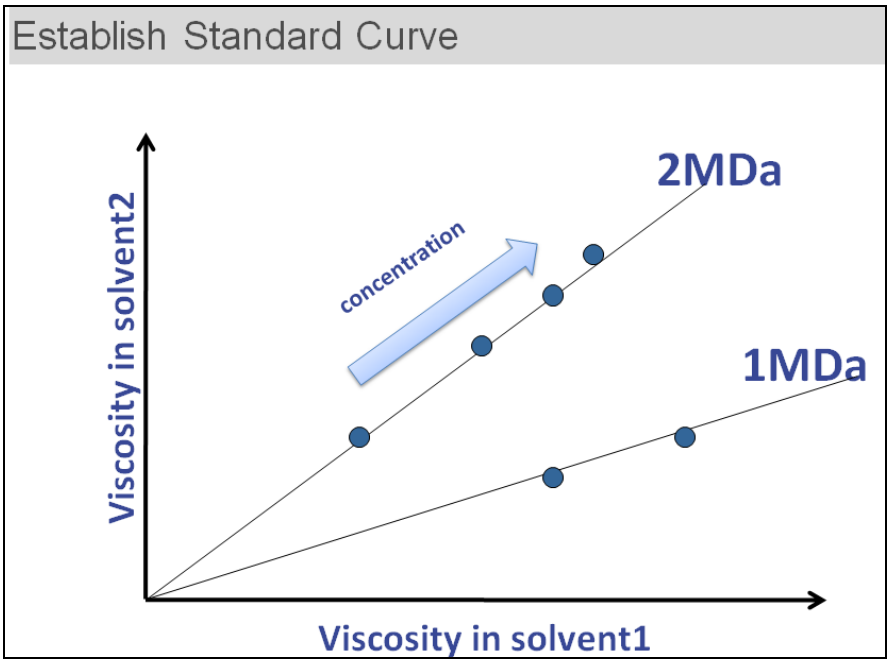

Figure 3-7: *The "standard curve" of viscosity in solvent 1(η_{sp1}) and viscosity in solvent 2 (η_{sp2}) for different molecular weights and concentrations*

Next, the polymer solution with unknown molecular weight and concentration can be run through the viscometer system under the same two solvent conditions. The resultant pair of specific viscosities of the polymer solution in each solvent may then be used to determine molecular weight. This process can be repeated for varying polymer concentrations of the same sample by changing solvent. This will provide another pair of specific viscosities, which can then also be used to determine same line passing through the same of higher concentration at the same molecular weight. Averaging the value of M for each of these different concentrations can then increase the accuracy of the result.

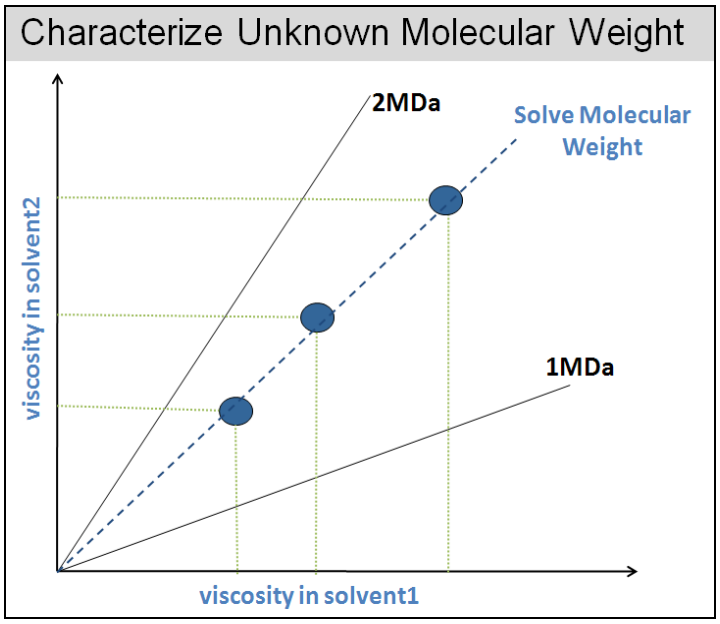

Figure 3-8: *Use of the standard curve to characterize an unknown molecular weight.*

3.2 The Microscale Molecular Weight Analysis System

The complete microscale molecular weight analysis system viscometer presented in this paper is composed of three modules: viscosity measurement, dialysis and post-processing automation software. The specific inputs and outputs to the system can be described in the following flowchart and table:

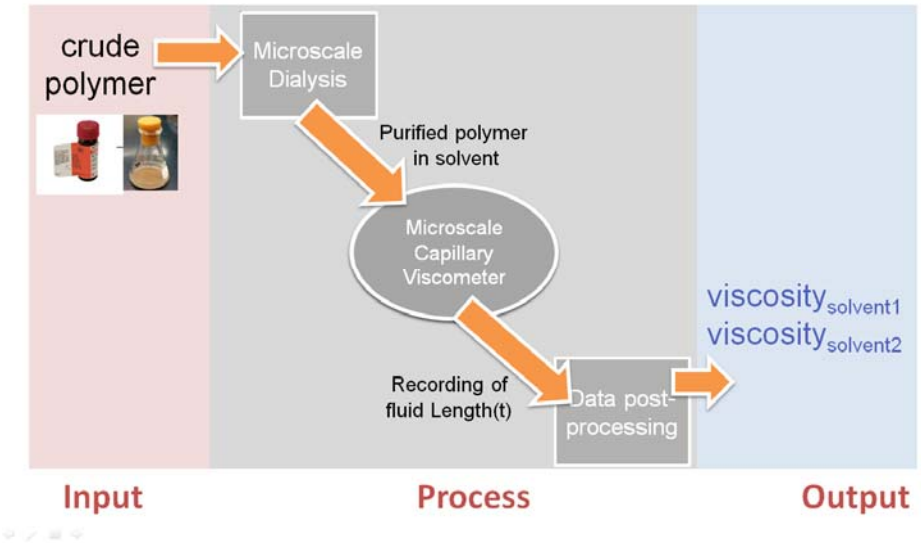

Figure 3- 9: *Composition of the Microscale Molecular Weight Analysis System and the inputs and outputs to each module.*

The microscale molecular weight analysis system is composed of three parts: a dialysis device for sample pre-treatment, the microscale capillary viscometer, and custom-written post-processing software.

The information in the flowchart is summarized with a brief explanation of the "mechanism" that allows each module to work:

Module	***Input***	***Mechanism***	***Output***
Microscale Dialysis	crude polymer solution: small molecular contaminants unknown solvent condition	Small-molecule diffusion, conductivity measurement	dialyzed polymer solution under known solvent condition
Microscale Capillary Viscometer	Polymer solution of unknown polymer concentration known solvent condition	Microscale Poiseuille flow	Recording of fluid Length as a function of time

Data Post-processing	Recording of fluid length over time	Image analysis	Viscosity pairs for a single known solvent condition

Table 3-5: *Modules of the microscale molecular weight analysis system*

The microscale capillary viscometer is the heart of the system. The principle behind this capillary viscometer will be discussed in this chapter and its efficacy and application will be discussed in Chapter 5. Its setup consists of a syringe pump attached to the outlet of the device using polyethylene tubing. The device is placed on the stage of a microscope, and the movement of the fluid within the device is recorded using a digital camera recording and stored on a personal computer.

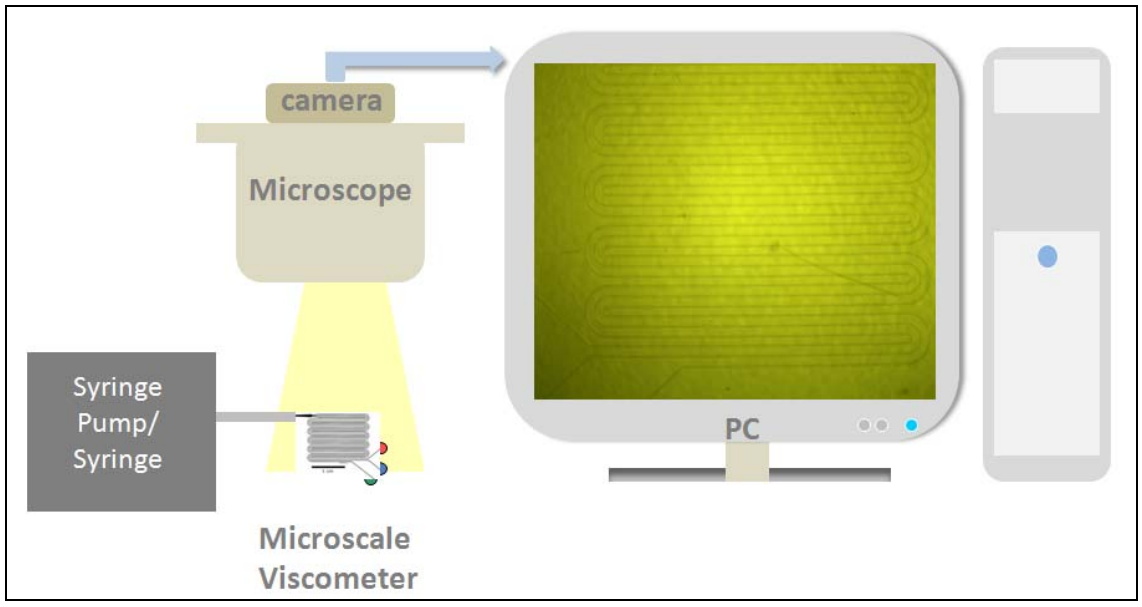

Figure 3-10: *Hardware setup for microscale capillary viscometer*

This recording is then processed and analyzed using automated image analysis software. This software examines the fluid lengths as a function of time and returns the corresponding specific viscosity values for each fluid stream. The hardware required for this module is the use of a personal computer and the encoded movie file.

Since the efficacy of the complete microscale molecular weight analysis method is dependent on using two specific solvent conditions, it is important to control the presence of small molecules from the solvent in the solution. In this system solutions can be pre-treated to add or remove salts using a dialysis device. The theory and applications of this dialysis system will be discussed in the following chapter.

CHAPTER 4

MICROSCALE DIALYSIS

Dialysis treatment is necessary when the concentration of ions in the sample polymer solution is unknown. In our device, the polymer solution is dialyzed by co-flowing it with a buffer stream of pure water or salt solution to change solvent conditions. The flux of salt ions into or out of the sample polymer solution is caused by the concentration gradient and the amount of diffusive transport can be adjusted by changing the flow rates through the device, or by changing the composition of the buffer stream.

This chapter will describe the theory behind the operation of the dialysis device, methods for verifying solvent conditions before and after dialysis, and the operation of the device itself.

4.1 Diffusion

Diffusion is the migration of matter down a concentration gradient. It can be quantified using the following relationship:

$$J_{A,z} = -D_{AB}\frac{dc_A}{dz} \tag{4-17}$$

where J is the flux, or the change in concentration of species A over the z direction, D is the diffusion coefficient of species A in solvent B, and c is the concentration of species A[34].

While convective forces dominate bulk fluid transport, diffusive forces can be dominant on the microscale. The diffusion of various molecules under specific solution conditions can be defined by the diffusion coefficient D_{AB} mentioned previously. As

expected, the diffusivity of a molecule is related to its size, or molecular weight. It can be roughly correlated as follows:

$$D_{AB} \sim \frac{1}{\sqrt{M}} \tag{4-18}$$

Where D is the diffusion constant of a high molecular weight polymer species A in a solvent composed of low molecular weight species B, and M is the molecular weight of the polymer species A[34].

The dimensionality of the diffusion coefficient from Fick's Law is $\frac{L^2}{t}$ and it is most typically expressed in the units of $\frac{m^2}{s}$. Thus the distance which a molecule will diffuse to over time can be expressed as:

$$x \approx \sqrt{2D_{AB}t} \tag{4- 19}$$

where x is the mean-squared distance the molecule will diffuse in centimeters, t is the residence time that the solute A spends in the solvent B in seconds, and D is the diffusion constant. This equation can be used with diffusion coefficients from literature to estimate the residence times required for diffusion of salt particles from a solution, while simultaneously keeping the polymer diffusion to a minimum. .

Diffusion is also often used with polymer science for dialysis. Fractions of polymer above a specific molecular weight can be isolated and purified by leaving a solution enclosed in a membrane with a known porosity. Small molecules such as salts and other impurities are then free to equilibrate by diffusing in or out of the pores, while larger polymer molecules remain within the membrane. Frequent changes in the solvent

or buffer surrounding the membrane enclosed solution then allow the removal of such particles. While this method is attractive for its low cost and versatility in adding or removing particles to a solution, it is time consuming due to the large volumes involved.

Here microfluidics offers a distinct set of advantages. At very small length scales and low flow rates, laminar co-flow of two streams allows two streams large contact areas to exchange small molecules via diffusion [35-38]. Since the length scale of these streams can be very small, the timescale for dialysis can be reduced. Also, flowing through a microfluidics device does not require the continual changing of static buffer in the case of dialysis bags.

Thus we have determined from this section that diffusion is a valuable tool that we can use for on-chip dialysis. The next sections of this work will discuss the design, construction, and testing of a microscale dialysis method to control solvent conditions.

4.2 Microscale Dialysis Device

The purpose of this microscale dialysis device is to add or remove salts and small ions using diffusion across two laminar co-flowed streams of polymer solution and within a long channel. Since flow is laminar, the two streams do not mix through convection, but exchange contents only through diffusion. The amount of diffusion which occurs is determined by the residence time, the amount of time which both streams spend flowing side by side, during which the streams flow side by side within the device. The devices have been designed to be long enough to have a residence time that allows complete diffusion of small ions to diffuse freely between the streams, but short enough to prevent the larger polymer molecules from diffusing. Design calculations were made using

estimates for salts and small molecules as less than 10 kDa in size with a diffusion constant of $10^{-9}\frac{m^2}{s}$ [34] and large molecules as greater than 1 MDa in size with a diffusion constant of $10^{-11}\frac{m^2}{s}$ [39].

The device, shown below, consists of two inlets, one for flowing polymer solution and the other for flowing buffer, and three outlets. A diagram of the device is shown below, along with a schematic of the setup used:

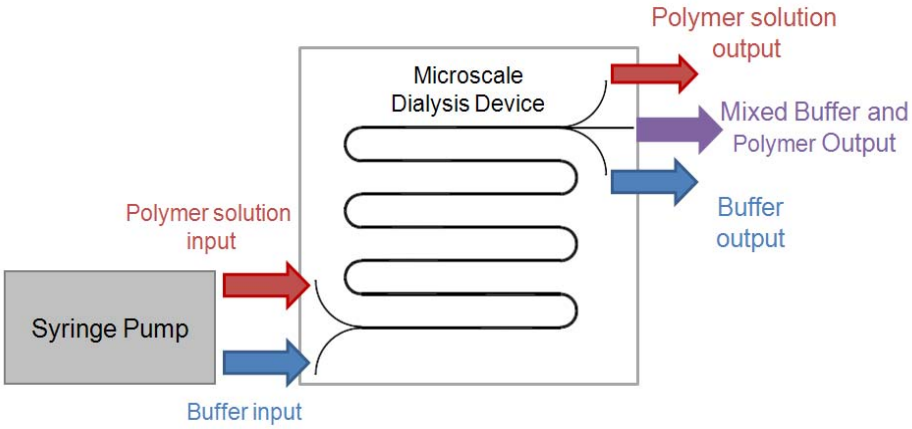

Figure 4-11: *The microscale dialysis device used in this study*

Since a small amount of polymer molecules can diffuse into the buffer stream, the concentration in the middle of the channel can be appreciatively lower than the input polymer concentration. However, by removing the middle section of the flow by providing an additional middle outlet, polymer concentration in the outer stream should remain.

In order to determine the operating regimes of this microscale device to control solvent conditions, it was necessary to devise a method to verify the condition of the

solvent before and after the treatment. To do this, our method employs solvent conductance measurements.

4.3 Measuring Conductance

Conductance is an important measurement for this project because it is used to measure the amount of solvent ions in a solution. Since our method is based upon specific polymer characteristics in two controlled solvent conditions of high and low ionic content, a measurement method is necessary to verify whether our solvent exchange in the dialysis device has worked. For this purpose, solution conductance proved useful to evaluate the salt content in solutions.

Electrical conductivity "*G* is a property which describes the solution's ability to carry electrical charges. A given object's conductivity can be described by:

$$G = \frac{\sigma A}{l} \tag{4-20}$$

where G is the conductance, σ is the material conductivity, A is the cross-sectional area, and l is the length of the object [40]. In this case, material conductivity was defined by the concentration of ions in the solution; higher concentration of ions in solution produced higher conductivity--and thus the higher conductance.

As with the rest of the system, conductance was measured using a microscale device. The conductance measurement device was a simple long channel of dimensions 12.5 cm in length, 50 microns in width, and ~80 microns in height made from a molded PDMS filled with the solution which had an unknown salt content. The channel was thoroughly perfused with a syringe such that one droplet extruded from the channel outlet, and another droplet of solution extruded from the inlet. Next, two 18 gauge steel wires of 4 inches in length were attached using alligator clips to a Fluke 179 multimeter

(Fluke, Everett, WA). Conductance could then be measured by taking the inverse of the solution's measured resistance. A figure showing the conductance measurement process is shown below:

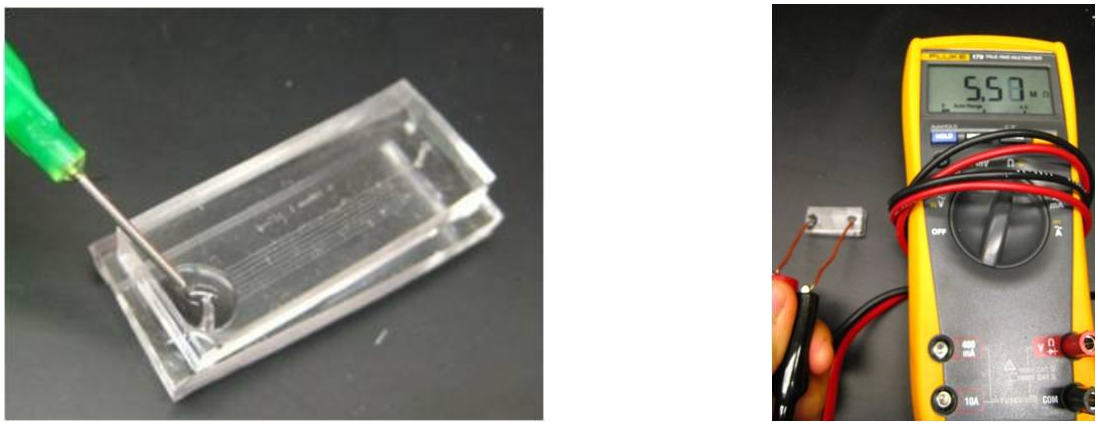

Figure 4-12: *Solution conductance measurement in a PDMS microchannel. Channel pre-filling (left) and the filled channel used to measure solution being used to measure conductance in a multimeter (right)*

Repeat measurements of a 0.45M solution of K_2SO_4 showed an absolute error of 0.2 Mega-Ohms. The results for the conductance of solutions of varying concentration from 0 to 0.5M K_2SO_4 and for 0 to 1.5M NaCl (Sigma, St. Louis, MO) are plotted below.

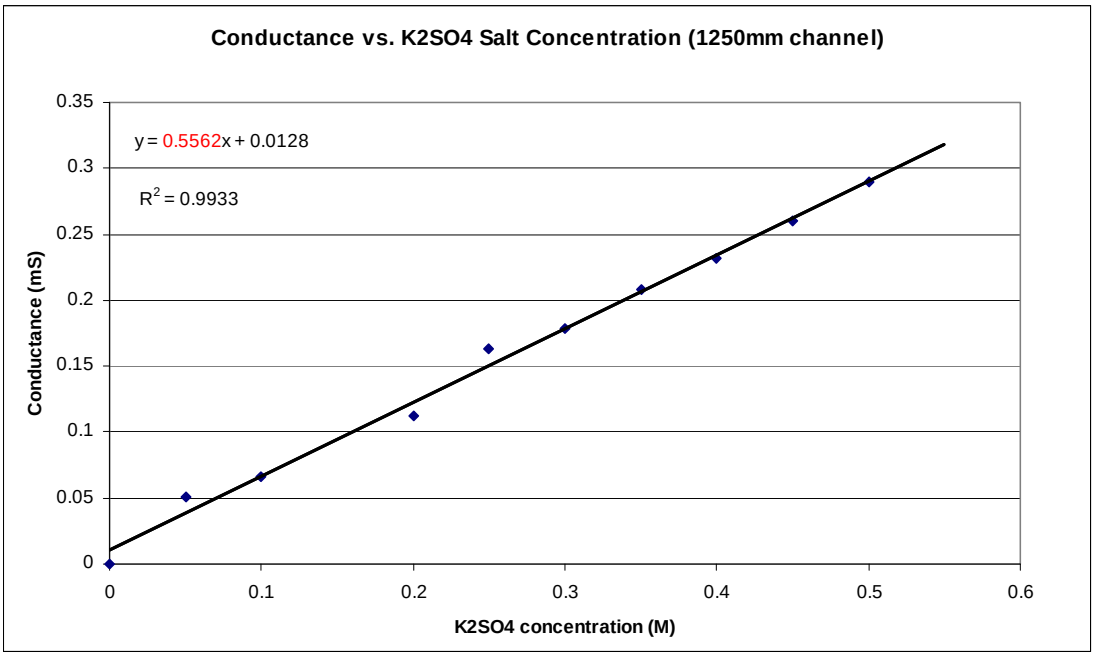

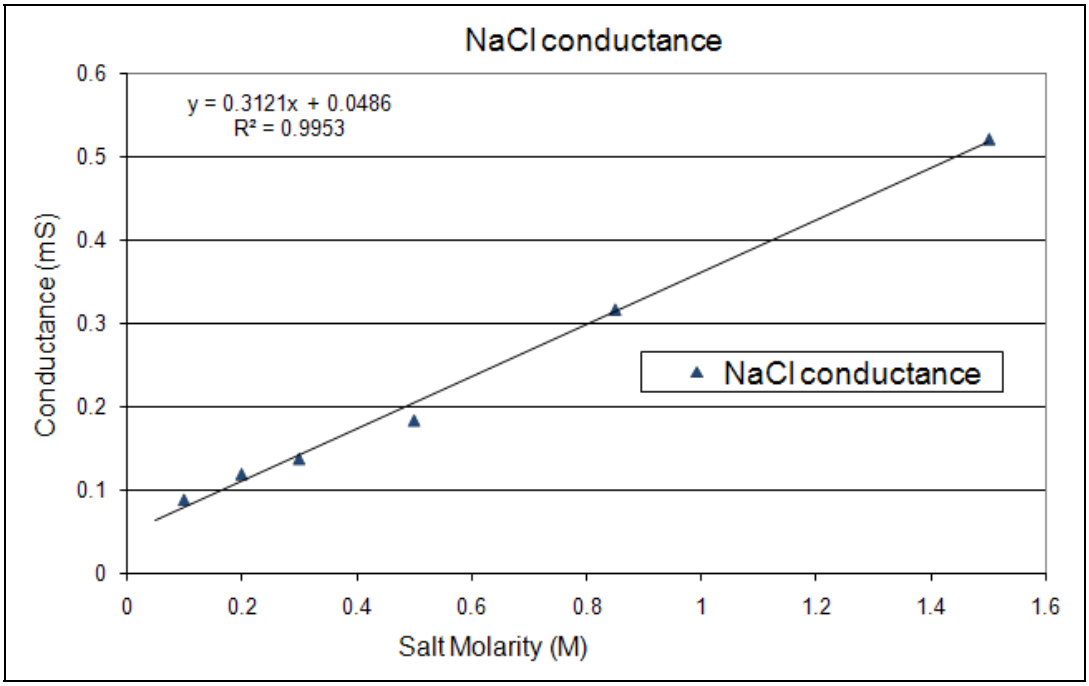

Figure 4-13: *Conductance vs. K_2SO_4 and NaCl Salt Concentration (both in 125.0mm channel)*

From these charts it is clear that for this range of salt concentration in the solvent, the conductance of the solution is linear with respect to the amount of salt ions in the solution and is not sensitive to the concentration of polymer in solution. The latter was

proven by repeat measurements of solution without polymer and solution with polymer, which showed the same conductance readings. Now that the theory and use of measuring the solvent conditions has been discussed, we shall turn our attention to the modeling and operation of the microscale dialysis module.

4.4 Modeling the Behavior of the Microscale Dialysis Device

The purpose of the microscale dialysis device is to be able to successfully remove small ions and impurities from the polymer solution sample and to redefine solvent condition. As mentioned earlier, the amount of salt that diffuses from one stream to another is based upon the residence time. One parameter that determines this residence time is the flow rate of both streams. To predict the efficacy of this device for different flow rates, a numerical model was constructed and analyzed. Modeling of both fluid movement and small molecule diffusion was performed on the finite element analysis program COMSOL (COMSOL, Burlington, MA), which was used to solve two sets of equations: the Navier-Stokes equation for flow and the diffusion- convection transport equation.

The model was constructed as a geometric approximation of the actual device. It has been scaled down in the x-direction and its outlets rotated to assist the program in solving the model. Specific boundary conditions used were: equal linear velocity (calculated from flow rate divided by channel cross sectional area width of 150μm multiplied by channel height of 200μm) at both channel inlets normal to the channels, fluid viscosities of 4 cP for the polymer solution and 1cP for the buffer solution, zero pressure at the device outlets, and no slip for all of the geometric borders except for those

corresponding to channel inlets and outlets. A normalized concentration of polymer was "1" at the top inlet and zero at the bottom inlet.

Since fluid viscosity and thus the flow streamlines are determined by the concentration of polymer at each point within the device, it is necessary to solve for fluid viscosity as a function of concentration. To do so, the model was solved by in a series of steps. First, viscosity was fixed at 1cP within the entire device, and the Navier-Stokes equation was used to solve for the flow profile (u,v,w) within the device. Next, this information on the fluid convection was saved and used to solve for the concentration gradient using the diffusion-convection equation, which produced values for concentration within the device. Third, the following equation defining viscosity as a function of concentration was used to simulate the viscosity differences of the polymer in solution and the buffer.

$$\mu = \mu_1 + (\mu_2 - \mu_1) * c \tag{4-21}$$

Here μ_1 and μ_2 represent the viscosity of the buffer and the polymer solution, respectively. In areas of the device where concentration of polymer was equal to zero, the viscosity is equal to that of the buffer alone, while in areas where the concentration of the polymer is the maximum value of 1, the viscosity is equal to that of the polymer solution alone. This function was then substituted for viscosity in the Navier Stokes equation, which was then solved to obtain the model of fluid flow within the device for solutions of different polymer concentration and viscosity.

The results of this modeling of the flow of polymer solution and buffer for microscale dialysis are shown below for flow rates from 5-20 μL/min.

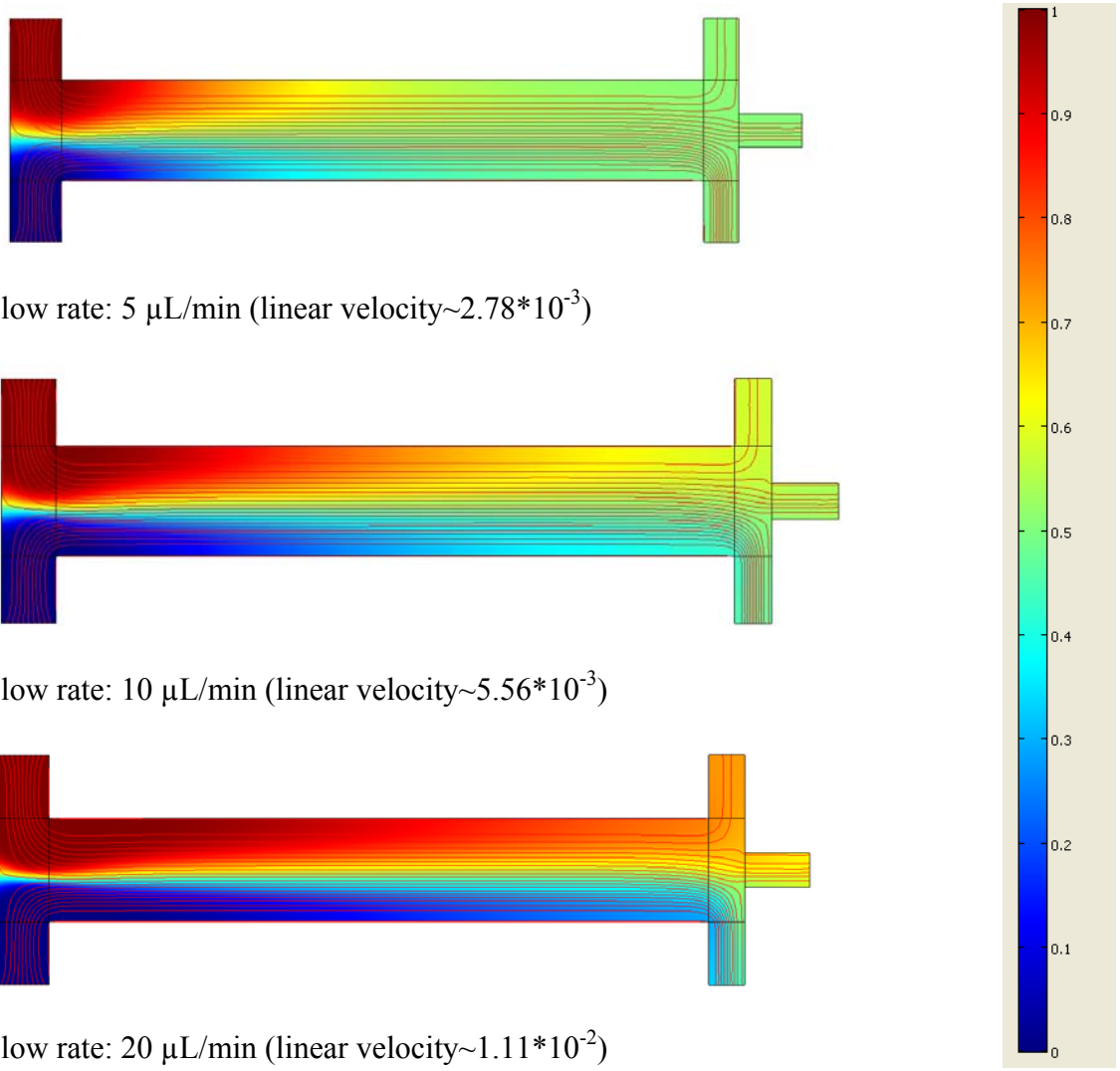

Flow rate: 5 µL/min (linear velocity~$2.78*10^{-3}$)

Flow rate: 10 µL/min (linear velocity~$5.56*10^{-3}$)

Flow rate: 20 µL/min (linear velocity~$1.11*10^{-2}$)

Figure 4-14: *Concentration of small salt ions (red at a maximum concentration of 1 to zero concentration in blue) and streamlines (indicated by red lines) for varying flow rates within the microscale dialysis device model.*

This model shows that the diffusion of molecules over both the polymer and buffer streams is complete for a flow rate of 5 µL/min (indicated by the green area at all outlets), but this diffusion diminishes as the flow rate increases to 20 µL/min. Thus for complete diffusion to occur, a flow rate of 10 µL/min or less appears necessary. Another observation that can be made from the model comes from the streamlines. The streamlines from the input channel at the top left of the device model of the more viscous polymer solution only come out from the top outlet channel. Thus we concluded that in order for diffusion to fully develop for small ions over this length scale, a flow rate of 5 µL/min should be used. The next step was to check that there was no significant polymer loss due to diffusion. To do this, the diffusion constant was changed to $D = 10^{-11}$, a literature value obtained from previous studies of the high molecular weight polymer dextran's diffusion in water [39].

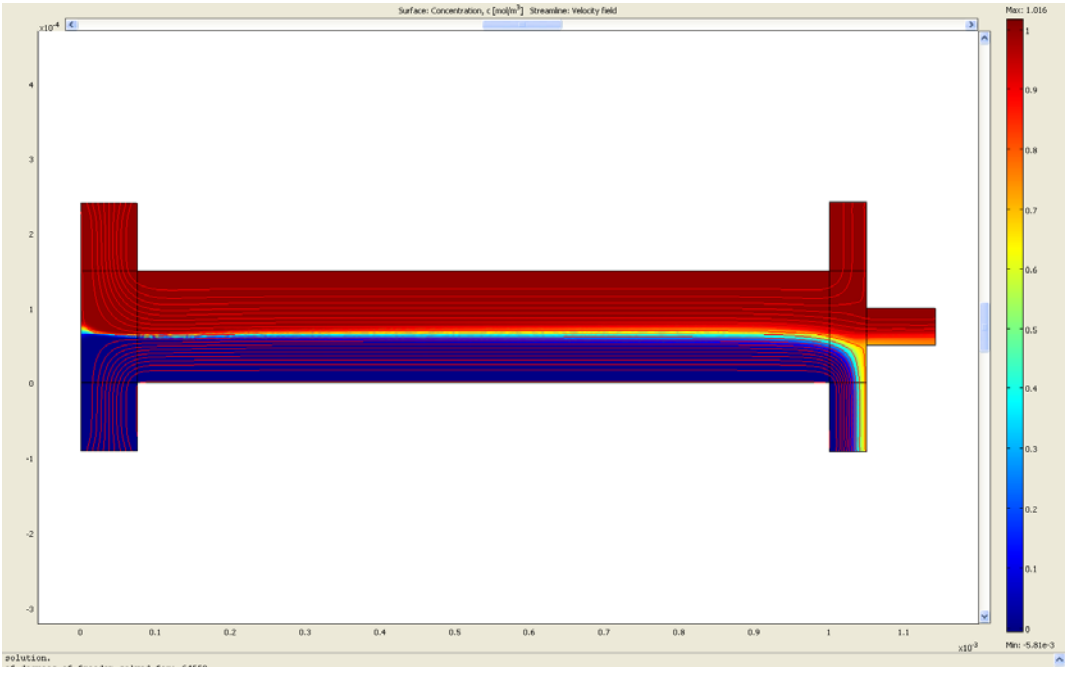

Figure 4-15: *Diffusion of high molecular weight polymer over the microscale dialysis device. Red indicates a relative concentration of "1" while blue indicates a relative concentration of "0".*

It can be seen from this model of polymer diffusion (relative concentration of 1 at the top indicated in red, and relative concentration of zero at the bottom left inlet indicated in blue).

4.5 Application and Results of Sample Pre-treatment

Results from the tests were analyzed using conductance of the effluent collected from each outlet channel. Each outlet was analyzed to ensure that the total concentration of salt removed from the device was equal to the amount entering.

In our experiment we co-flowed pure water and polymer solution with each other in the device at a flow rate of 5 μL/minute for a total volume of 1.5mL. The resulting conductance was converted to a salt molarity using the standard curve for NaCl established in 4.3.3. This molarity was then converted to a number of moles based on the volume of the effluent of each channel. The results are shown below for the average values of n=3 trials:

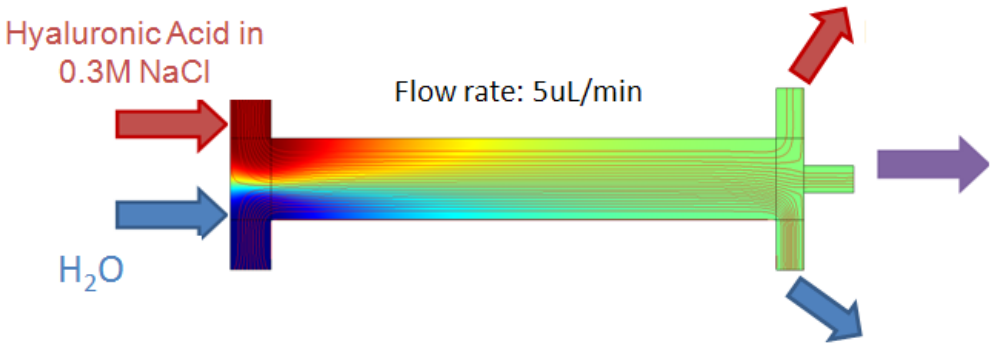

Experimental microscale dialysis results averages from (n=3)

NaCl in (mols)
Top: 6.0e-4
Bottom: 0
Total: 6.0e-4

NaCl out (from conductance)	
mol fraction	mols
Top: 32%	1.2e-4
Middle: 30%	1.2e-4
Bottom: 37%	1.5e-4
Total	3.9e-4

Figure 4-16: *Results of experiments on the microscale dialysis system*

These results show the efficacy of this dialysis system in two ways. First, the mole fraction of effluent is similar over all channels, indicating that the equal concentration prediction was correct. Second, the number of moles of NaCl in is on the same order of magnitude as the total number of moles exiting the device. We interpreted this to indicate that the conductance measurements of molarity were correct to an order of magnitude. The conductance measurement technique has the potential to be more quantitative, and future work should focus on better defined electrodes and experimental setup.

Thus we concluded that the diffusion behavior of the dialysis device was correctly predicted by the COMSOL model. For the a flow rate of 5 µL/min the residence time of the stream carrying polymer and salt molecules co-flowed with a buffer stream of water stream was sufficient to allow complete diffusion of small salt ions over both streams.

This section has shown the design, computational modeling, and application of the microscale dialysis system of sample pre-treatment. In this work, all trials of this microscale dialysis device were performed separately from the viscometer module, which will be discussed in the next chapter, to make it easier to troubleshoot each device. Since one of the primary goals of this system is to characterize molecular weights for very small volumes and low concentrations under stringent solvent conditions, a similarly microscale method for dialysis is necessary. Thus the eventual use of polymer solution purified using this microscale method together with our viscometer is an issue that needs to be addressed in future work.

CHAPTER 5

MICROSCALE CAPILLARY VISCOMETER

This section will first discuss the theory behind the operation of a capillary viscometer. It will then show how this theory can be implemented into a microscale viscometer. Previous microscale viscometers will be discussed, along with their evolution into the new design from this work.

5.1 Theory

Capillary viscometry measures viscosity by observing the laminar flow of a fluid through a tube [41]. This type of flow can be described as follows:

$$\Delta P = \eta \frac{SvL}{d_h^2} \tag{5-22}$$

In this relationship, known as the Hagen-Poiseuille equation, the radius (for a tube with circular cross-section) or the hydraulic diameter d_h^2 (for a tube with rectangular cross-section) is much less than the length, L. With this equation it is possible to determine fluid viscosity by examining the velocity of a length of fluid over time for a given pressure gradient within a thin tube of known dimensions.

Capillary viscometers are commonly used pieces of lab equipment that uses the Hagen Poiseuille equation to calculate viscosity. In these viscometers, a fixed volume of fluid is dispensed into a reservoir between graduation marks. The fluid is then driven by pressure head to flow down into a thin glass capillary. Since the driving pressure is assumed to be only due to height and gravity, the viscosity can be measured as:

$$\eta = tx\rho \tag{5- 23}$$

where t is the time that the fluid takes to flow down the capillary and ρ is the density of the fluid, which for dilute solutions is often assumed to be 1 [41].

5.2 Previous Microscale Viscometry Technologies

Small-volume viscometric analysis methods have a number of important biological applications. Biological samples such as blood, urine, and saliva are routinely screened in hospitals. Viscosity-related features of these fluids are key indicators of a number of economically important diseases such as diabetes, anemia, heart disease, and various blood-borne infections. Thus it is clear that the development microscale viscometry has a number of high impact applications beyond metabolic engineering and polymer analysis.

Currently the Canon-Ubbelohde capillary viscometer is one of the most popular tools for macroscale analysis of solutions. Recently, it has been adapted into microscale forms both in silicon [42-45] and in poly-dimethyl-siloxane (PDMS) [46], and shall be further discussed. Other microscale methods presented for measuring viscometry include examining the interface between two fluids in laminar flow [47] and a Wheatstone Bridge-based differential fluidic resistance detector [45]. The next part of this section will describe the development of the Ubbelohde capillary viscometer into a micro-scale device.

The capillary microscale viscometer has been primarily developed by two groups, Srivastava *et al* [42-44]. and Han *et al* [46]. The capillary viscometer discussed in this

work is based upon their work, but has been altered to improve throughput, and increase the ease and repeatability of fluid actuation on the device.

5.2.1 Microscale Glass Capillary Viscometer by Srivastava *et al.*

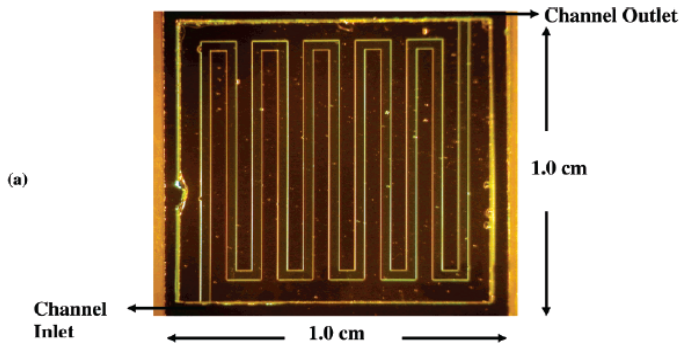

Figure 5-17: *Srivastava et al. viscometer, first generation*

The first microscale capillary viscometer known by the author was constructed by Srivastava *et al.* as a single channel capillary fabricated using glass etching techniques [42]. In this device, fluid flow in the device was initiated spontaneously after the placement of a microliter-scale sample droplet outside of the device. This spontaneous entry was made possible by two factors: the relatively large size of the sample droplet radius compared to the size of the sample interface within the micro-channel and the hydrophilic character of the glass surface of the device pulls in aqueous solutions. The pressure drop on the fluid from the outside sample to the inside can be derived from the definition for LaPlace pressure and defined within this system as:

$$P_{cap} = 2\sigma \cos\theta(\frac{1}{d} + \frac{1}{w}) \quad (6\text{-}24)$$

In this system P_{cap}, the pressure drop from the outside of the device to the inside of the device, is calculated through experimentally determining the wetting angle θ for the known parameters surface tension σ, and d and w are the depth and width of the micro-channel respectively. For a glass channel with a small wetting angle, it is apparent that the $\cos\theta$ term approaches 1 and the capillary pressure is large. This large difference in capillary pressure outside the channel vs. inside of the channel is sufficient to pull fluid into the channel and initiate flow. This method of capillary pressure induced flow is advantageous because it does not require external forces to conduct measurements.

Drawbacks to this device model were that the single-channel nature of the device required that four measurement chambers to determine an absolute viscosity. This was due to notable heterogeneities in the dimensions of each of the glass devices, which the authors attributed to the fabrication process. Differences in fabrication also affected the device-to-device reading variability. Control readings for the viscosity of water varied by 22%, although the average over 25 devices was accurate compared with literature. Another drawback to the device was the high cost in time and materials and the use of harsh chemicals involved in the glass microdevice fabrication process.

5.2.2 Microscale PDMS Viscometer by Han *et al.*

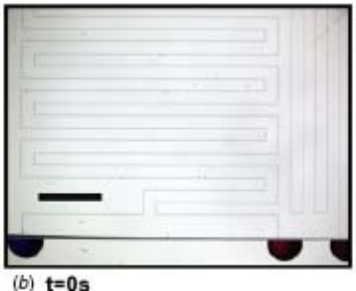

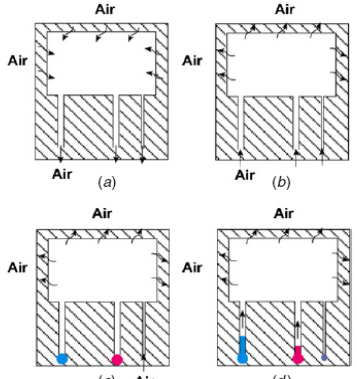

Figure 5- 18: *schematic and device for PDMS viscometer from a previous design by Han et al.[46]*

More recently, a microscale dual-channel viscometer was developed in PDMS[46]. Since PDMS is a non-wetting material, its wetting angle θ is large, and thus the pressure difference from capillary pressure alone is insufficient for fluid to spontaneously wet the channel. Thus pressure actuation of fluid into the channel had to be achieved by an external force. This was provided by removing the air within the PDMS of the device using a vacuum dessicator and removing it right before use. Directly after removal from the dessicator, sample drops were placed at the entrance of the channels. Due to the porous PDMS of the device, air was still being pulled from the channels into the PDMS walls of the device after vacuum treatment. Thus the channels exert a driving pressure difference that actuates fluid flow.

In addition to providing a different method for creating flow, this viscometer also employed a two-channel design that prevents the need for separate calibration measurement. This method is discussed more in depth later in this section.

Drawbacks to this design include the need for the time-consuming and inefficient process of vacuum sealing each device before use. For each device, vacuum dessication took about 12 minutes while the measurement of fluid viscosity took about 4-5 minutes.

5.3. First-Generation Viscometer

The first generation viscometry devices designed in this work attempted a straight, parallel channel configuration since such a design could be easily expanded to

Due to their straight geometry, all three devices had a limited area which could be observed under a microscope. The largest field of view obtainable for this system was approximately 3cm by 2.5 cm. This meant that the longest region of channel that could be observed was about 3.9cm. This length of channel proved insufficient for all three devices for obtaining a level of resolution greater than or equal to the standard set by the PDMS viscometer created by Han *et al.*

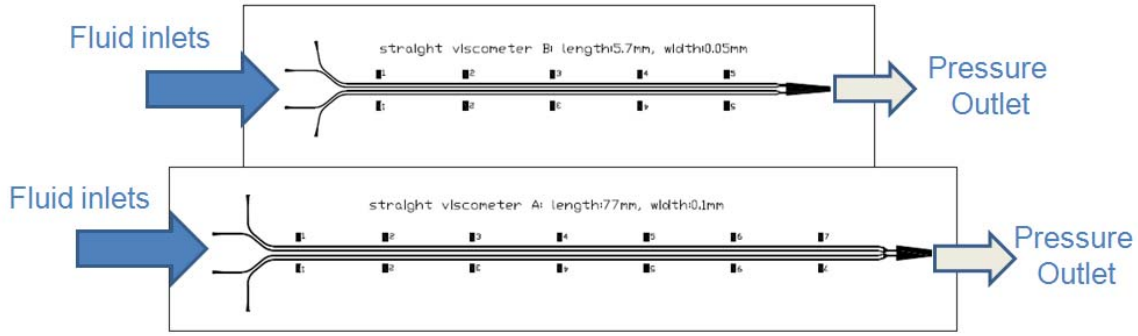

***Figure 5-19**: First generation of straight-channel viscometers*

There were three designs evaluated in the first round. The first of these had the smallest aspect ratio of 200 microns wide to 2cm long. Due to this low aspect ratio, the resistance of the channel allowed fluid to move quickly through the channel. Unfortunately the fluid moved too quickly to measure appreciable resolution in preliminary control experiments with water and 10% glycerol.

Given the outcome of this first device, the second and third straight channel devices attempted to reduce the speed of flow so that differences could be measured with a high level of resolution. To do this, the channels were modified at their entry to taper from an opening twice as wide as the channel. This would decrease the initial drop in the size of the interface going from outside the channel to inside the channel, thus allowing

the fluid to be actuated at lower pressures and subsequently lower speeds. Another method for attempting to uniformly increase the affinity of the water for the device channel was to modify the surface of the PDMS.

5.3.1 Surface Treatment

Coating the PDMS surface for a straight-channel viscometer was an attractive goal for a number of reasons. First was that the sufficient decrease in capillary pressure due to surface treatment could help fluid uniformly enter the channels and thus negate the need to use other devices to create a pressure gradient sufficient to initiate flow, such as the syringe pump used in the current device. Another reason that the surface coating was desirable was to prevent the adhesion of polymer to the inner surface of the channel. PDMS has previously been documented to have fouling issues with microbial cultures due to their hydrophobic extracellular polysaccharides [48]. Since one of the goals of this device is to examine to production of such polysaccharides, this problem was one of significant concern. Thus the coating was implemented to prevent adhesion, and to enhance the wetting characteristics of the channel to allow a slow, smooth flow which could enhance the observation of differences in fluid viscosity. The protocol for hydrophilic PDMS channel coating was taken from Ebara *et al.*'s process for coating PDMS channels using polyethylene-glycol diacetyl (PEG-DA) [49]. The process was as follows:

1) First devices were fabricated in PDMS and plasma bonded to PDMS slabs. These were then left over two days to resume their native hydrophobic state.
2) Next a pre-polymerizing agent, benzophenone dissolved into acetone, was flowed into the channels. Due to its hydrophobic nature, the compound easily adsorbed into the PDMS of the channel.
3) Third, the channels were rinsed with water to prevent polymerization within the channel.
4) Next, the PEG-DA was dissolved into a solution of benzyl alcohol and water, and flowed into the channels until all were filled.
5) The solution within the device was then exposed to an ultraviolet light source (100 watts, 365nm wavelength, 5cm from the light source), graciously provided by the Temenoff lab and Taymour Hammoudi, for ten minutes. For devices larger than the focal area of the lamp, each area was exposed for ten minutes. The combination of pre-polymer benzophenone on the surfaces of the PDMS channel, along with the PEG-DA and benzyl alcohol solution creates a photopolymerized, hydrophilic PEG-DA coating on the surface of the channel.
6) Finally devices were rinsed thoroughly and left overnight before testing.

Four devices were treated using this method. Although treatment was shown to make the channel hydrophilic, the surface treatment was observed to be nonuniformly distributed through the channel. When assayed for viscosity readings through recordings of fluid flow through the channels, the flow was still too fast and too uneven over the

small area of the straight channel that could fit in the maximal area of the plane of the microscope.

Another problem was that the coating was not effective for this device due to its non-equal coating amongst each of the channels. This was observable from examining the channels walls after blowing air through the device. In an uncoated channel, all water is generally removed after pushing ~10mL of air through the device. In contrast, in these devices water was observable in only two out of the four channels. This contrast is shown in the figure below:

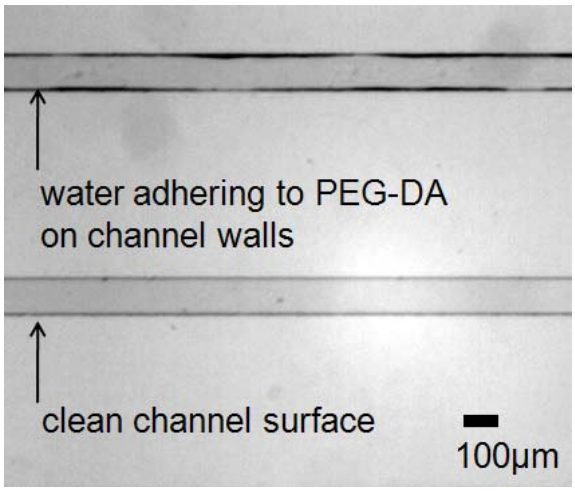

Figure 5-20: *Uneven hydrophilic coating of channels after PEG-DA treatment*

Additional evidence for uneven channel coating using this process was that two of the four viscometers treated showed spontaneous fluid movement into some, but not all channels of the viscometer, although this could have been due to inconsistencies in cutting open the channels on the PDMS device layer. The final problem with this PEG-DA coating was that its effects visibly degraded over continual use. This could be observed by the decrease in magnitude and frequency of spontaneous fluid motion into the channels. Since one of the original purposes was to increase overall device

reusability, this was a salient issue. Due to these shortcomings, this technique was abandoned and changing the pull rate of the syringe was found to compensate for surface effects due to re-use.

5.3 Current Generation Viscometer

The microscale capillary viscometer device design used in this work is also a multi-channel device fabricated from PDMS. This design has improved upon previous designs by increasing throughput and by using more rapid and reliable method for fluid actuation.

This device is different when compared to other microscale capillary viscometers in its method of fluid actuation. Since the device is fabricated from hydrophobic PDMS, actuation by spontaneous wetting is not an option. However, the previous method of vacuum desiccation was not as convenient for regular laboratory use. Thus this device instead uses an external syringe pump to provide a controlled negative pressure to generate a sufficient pressure difference between the sample outside of the device and the air inside the device to pull fluid inside. A schematic is shown below:

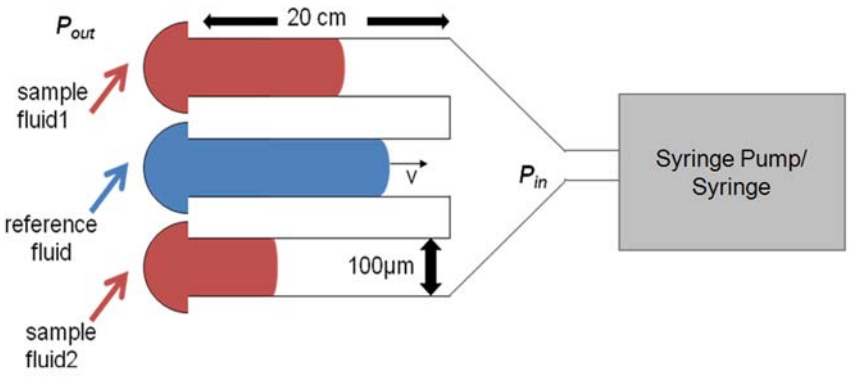

***Figure 5-21**: Schematic for pressures within device*

This method of negative pressure generation is faster to apply than the desiccator and allows the user to define the amount of pressure applied. Finally the use of the syringe pump negates the need for a large on-chip pressure chamber, giving the PDMS device itself a much smaller footprint than previous designs.

Pressure control was also importance for preventing fluid velocities which were too low, too high, or changed too much over time. High pressure differences created high fluid velocities that would exert large shear forces, which can cause shear thinning in high molecular weight polymer solutions [29]. Alternatively, at low pressures differences, the resultant slow fluid flow could increase the effects of surface irregularities by deforming the fluid meniscus [50].

The basic operation of this device can be described as follows. First the pressure difference between the fluid inlets and the pressure outlet, which initiates flow in all channels of the device. Next the speed of the fluid and the length of the fluid "plug" within the channel over time are recorded, and viscosity is calculated from this data.

Flow within the viscometer can be described by the equation for Poiseuille flow for both the reference fluid ("r"), and the sample fluid ("sample"), as seen below:

$$\Delta P_r = \Delta P_{cap\_r} + (P_{in} - P_{out}) = \frac{S\mu_r v_r L_r}{d_h^2} \tag{5-25}$$

$$\Delta P_{sample} = \Delta P_{cap\_sample} + (P_{in} - P_{out}) = \frac{S\mu_{sample} v_{sample} L_{sample}}{d_h^2} \tag{5-26}$$

Here ΔP is the total pressure drop, ΔP_{cap} is the pressure drop due to capillary pressure, S is a shape constant, v is the speed of the fluid, and L is the time dependent length of the fluid plug within the channel from the entry of the channel to the moving

fluid front. It can be seen from these two equations that when P_{in} and P_{out} are the same for both the sample and the reference fluid. Thus they can be combined into a single expression:

$$v_r L_r = \frac{\mu_s}{\mu_r} v_s L_s + \frac{\left(\Delta P_{cap\_r} - \Delta P_{cap\_s}\right) d_h^2}{S\mu_r} \tag{5-27}$$

This equation has been derived earlier from the previously discussed works of both Han and Srivastava.

The driving pressure difference in this device is generated using a syringe controlled by a syringe pump. The syringe is attached using a Luer stub and Teflon tubing (Scientific Commodities Inc, Lake Havasu City, Arizona) to a central chamber. As the syringe pump (Harvard Apparatus, Holliston MA) pulls the plunger of the syringe backwards, the volume of the syringe increases, and thus the pressure inside decreases. Thus the pressure inside the device (P_{in}) is much lower than the combination of the outside atmospheric pressure (P_{out}) and the added difference in capillary pressure (P_{cap}).

Our delivery scheme using the syringe or syringe pump is an improvement from previous work because unlike previous models it allows for the rapid reusability of devices and allows for a chip with a smaller "footprint". It also allows greater control over the pressure difference at either end of the fluid, and thus the rate of fluid flow through the viscometer. This control over the pressure difference could allow future work on examining other fluid characteristics, such as sensitivity to different shear forces under greater pressure differences. In low-budget, or point-of-care situations, this device could also be adapted to work with a small hand-held manual syringe, reducing the overall equipment cost and increasing portability.

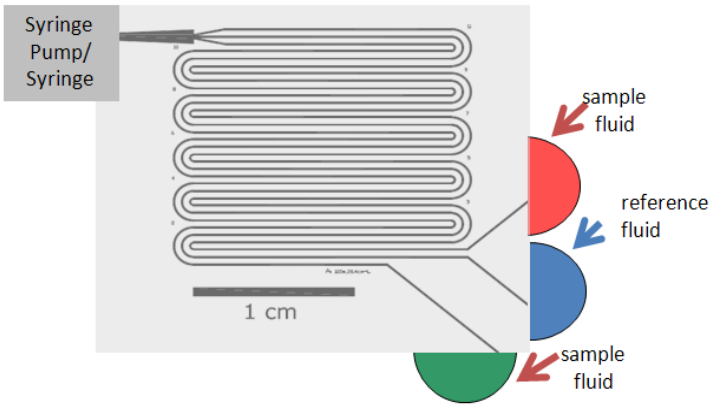

Figure 5-22: *A schematic of the current device operation*

This generation of devices differs in geometry, number of channels, and lack of surface treatment. The geometry of this device is three very long, curved channels placed next to each other. The curved nature of these channels was necessary in order to fit as much area as possible onto the field of view of the microscope. The curved channel design allowed a much larger observable channel region of 19.5 cm for each channel compared with the 4cm observable channel region on the straight channel. The radii of curvature used were chosen to maximize the amount of channel visible under the microscope, allowing good resolution between the three channels. Although the top and bottom channels have alternating radii of curvature while the middle channel has a single radius of curvature,

This device also employed curved turns instead of square turns (as in the device of Han *et al.*) to prevent the accumulation of air bubbles reported by previous groups [44, 46]. This choice of curved vs. square geometry has investigated previously and found to have no significant effects on viscosity readings from the devices [44].

Another factor for consideration in the design and fabrication of this device was the shear rate experienced by the fluid in the channel. This is important to assess whether fluids measured experience very high levels of shear. To estimate shear levels, the following equation was used:

$$\dot{\gamma} = \frac{dV}{dy} \approx \frac{l/t}{h/2} \tag{5-28}$$

In this approximation, a parabolic velocity curve is assumed such that velocity at the wall of the channel (y=0) is zero, and the velocity at the center of the channel (y=h/2) is the average velocity, which can be defined as the length of the channel over the time for the fluid to flow that distance. By this estimate, the shear rate within the channel is approximately $67s^{-1}$. This low level of shear is within the range that is reported to have no shearing effects on dilute amounts of the PEO polymers greater than 1MDa in molecular weight [4, 19].

To test the effect of curves in the channels on the accuracy of the device's results, viscosity was first calculated using all points within the channels. This was then compared with the viscosity calculated by taking only the points in the straight parts of the channel. The reference channel was loaded with Millipore water, and a sample channel was loaded with a dilute concentration of polyethylene glycol (MW = 10,000Da). As in all subsequent experiments, pressure was delivered by the syringe as 0.8 mL initial volume removed followed by a volumetric refill rate of 500uL/minute. Results are shown below:

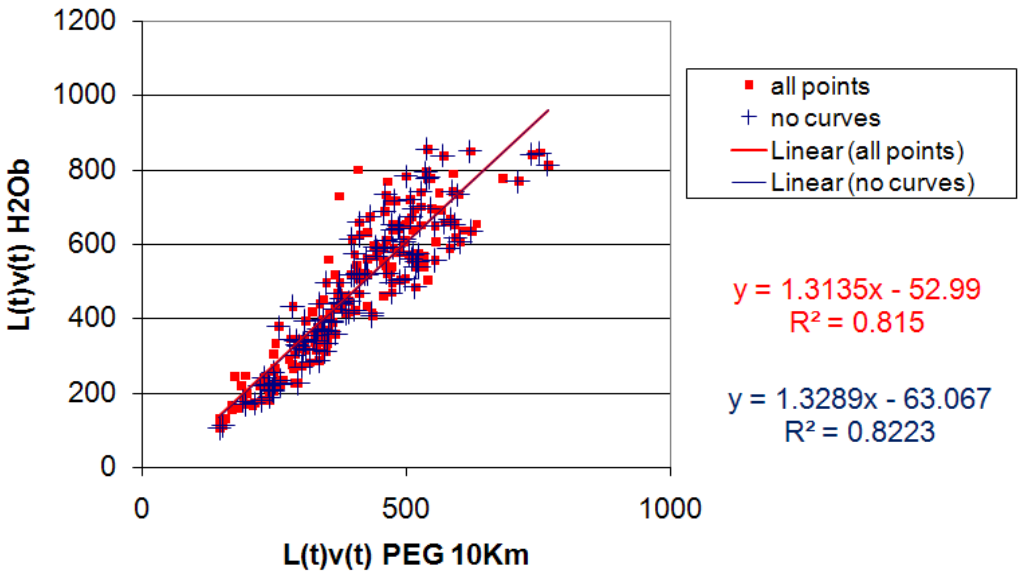

***Figure 5-23**: Effect of curves in viscometer channels on viscosity measurements*

Calculated value of the viscosity (the slope of the graph shown) showed less than 5% difference in measurements. This was found to be true for three other samples treated in the same way. Thus it was concluded that the difference between the inclusion of all points vs. that of the curves does not significantly impact the measurement of viscosity.

Finally the device itself and an example of its operation can be seen below:

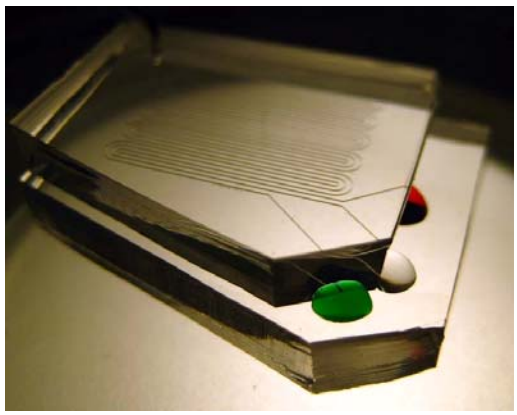

***Figure 5-24**: PDMS capillary viscometer with sample fluids (dye)*

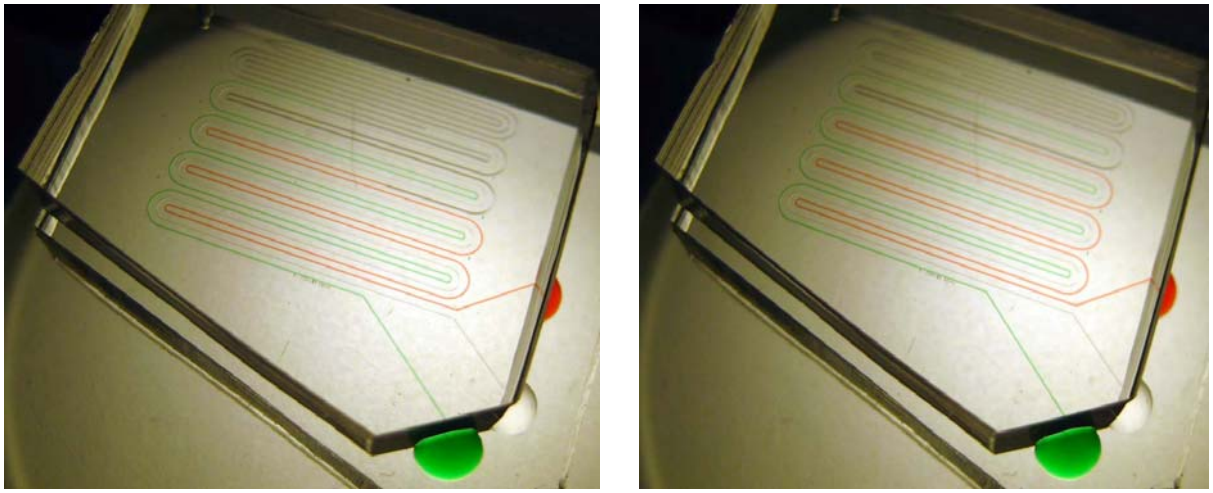

Figure 5- 25*: Device at time t1 (left) and slightly later at time t2 (right). Clear fluid is water reference while the green and red dyed fluids are aqueous solutions of 10% and 30% glycerol, respectively*

5.5 Device Fabrication

The microscale capillary viscometer devices used in this study were created using well-established techniques for single-layer devices made from PDMS[51]:. The following procedure was used

1) First, the design for the device was drafted in AutoCAD (Autodesk, San Rafael, CA). The drawing was then sent to a printing service for the creation of a high resolution photomask. The photomask drawing is shown in the Appendix of this work.
2) The device was then fabricated using soft lithography molding techniques [52]. Briefly, a silicon wafer was first dried using a hotplate to remove moisture. Next, a layer of the negative photoresist SU-8 2050 Microchem (Newton, MA), was spun onto the surface of a silicon wafer. According to data from the manufacturer the layer should correspond to a feature height of approximately 80 microns. The SU-8 layer was then exposed to ultraviolet light for polymerization.

3) Using the Silicon master mold, devices were then patterned by pouring Poly-Dimethyl Siloxane (PDMS) onto the wafer and baking for 2 hours at 70°C. The PDMS was composed of Sylgard 184 elastomer and cross linker (Dow Corning, Midland, MI) and mixed in a ratio of 10:1.
4) Devices were cut such that the inlets were open to the air within 20-50 microns of the end. Due to the very long overall channel length (~19.5 cm) small variations in the length of the cut ends were negligible. Outlet holes were made using a 19gauge luer stub. Next, the devices were cleaned using 3M Scotch tape and compressed air, then plasma treated for 30 seconds. The devices were then bonded to PDMS. After bonding and cleaning, devices were left overnight at 70°C to allow the PDMS surface to regain hydrophobicity [53], which prevents fluids from wetting and entering the channel without external pressure exertion.

The PDMS silicone elastomer is an excellent platform for biologically studies because it is optically transparent, non-toxic, and easy to use in device fabrication. Its primary material properties include its hydrophobicity and bulk porosity.

5.6 Viscosity Measurement Controls

The microscale capillary viscometer evaluated in this work is the keystone of this the proposed method. Thus, this chapter show and discuss the efficacy of the developed device at evaluating the fluid viscosities of various polymers. First it will show the results of low molecular weight controls, and then it will be used to evaluate high molecular weight polymers. Results will be compared to literature values and macroscale methods.

Testing began with control trials to ensure the accuracy of our viscosity measurements. After the device-to-device and channel-to-channel controls showed non-significant variations, the viscosity of low molecular weight polymers was compared with existing literature data. Finally, the device was used to evaluate the viscosity of high molecular weight polymers in solution and the results were compared with existing literature.

The first control tests that were run evaluated the channel-to-channel variation within the three channels of the viscometer device. This was achieved by flowing water in all three lanes and measuring their respective viscosity measurements relative to each other. Specifically, we measured the $\eta_{rel} = \frac{\eta_{channel\,1}}{\eta_{channel\,2}}$ of the water and considered the resultant percent standard deviation from "1" to be the most accurate measure of the variation. For thirty measured trials of Millipore water in the first and second channels the standard deviation of the readings was 1.75%, providing a baseline of error for all of the subsequent experiments. Sources of this error might include small irregularities in device fabrication and in software automation of viscosity readings. Before use, all devices undergo the aforementioned control test with water in all three lanes. Devices with standard deviation rates above 2% for their lanes in water controls were discarded. Causes for non-uniform channel-to-channel variation included the presence of dust in channels, and a poor seal between the pin connecting the syringe pump to the pressure outlet of the device.

The next set of controls executed examined viscosity measurements for various low molecular weight compounds. For these trials, four microscale capillary viscometers were molded from the same patterned wafer, used for measurement, cleansed, dried, and

re-used. In operating the devices, the initial volume of air removed by the syringe pump was 0.8mL, after which a fixed rate of 500 µL/min was drawn out of the device. Movies were analyzed using the first generation Matlab program. Small molecule solutions chosen were varying concentrations (10%, 30%, 50% w/v) of glycerol and sucrose (5% w/v). The resulting measurements were compared with a macroscale Ubbelohde viscometer at the same room temperature of 24°C.

Sample	Microscale Viscometer (η_{rel})	Macroscale Viscometer (η_{rel})	Error: microscale vs. macroscale
Glycerol 10%	1.322 +/- 0.054 (n=5)	1.357 +/- 0.053 (n=3)	0.03
Glycerol 30%	2.364 +/- 0.011 (n=3)	2.657 +/- 0.027 (n=3)	0.29
Glycerol 50%	6.22 +/-.049 (n=3)	6.272 +/- 0.005 (n=3)	0.05
Sucrose 5%	1.072 +/-0.02 (n=3)	1.103 +/- 0.005 (n=3)	0.03

***Table 5-6**: Measured small molecule viscosities with comparison data from macroscale Ubbelohde viscometer [46, 54, 55]*

The validity of the viscosity readings was measured by the percent error from literature, and from the standard deviation of the readings. The latter was important for experiments in which relevant specific conditions such as temperature and the type of viscometer used of the viscous measurement are not mentioned or cannot be precisely matched.

5.7 Device Re-Use

Another area which was investigated was the possibility of device re-use. This was significant since each wafer allowed only four devices to be made per round of fabrication. For re-use to be viable, we investigated the possible effects of polymer adsorption on viscosity readings. Another reason this was examined was because

adsorption could cause a decrease in polymer concentration at the front of the fluid vs. at the entry of the channel to which the polymer had adsorbed. Since the polymer solutions in this work exist at dilute concentrations, any surface adsorption would cause significant changes in viscosity.

To see if surface adsorption changed the viscosity readings, we evaluated changes in our system's viscosity measurements over a number of device re-uses. We hypothesized that the first use of the viscometer would have the most significant adsorption issues. Over subsequent uses, more polymer would adsorb to the capillary walls until no surface sites remain for the polymer to coat. Thus if adsorption occurred, viscosity measurements would change over the first few readings, and then level out over increased uses. Since PEG 10K was a compound observed to coat the inner surface of the viscometer after its usage, we used it as a test model. The results of these tests are shown below:

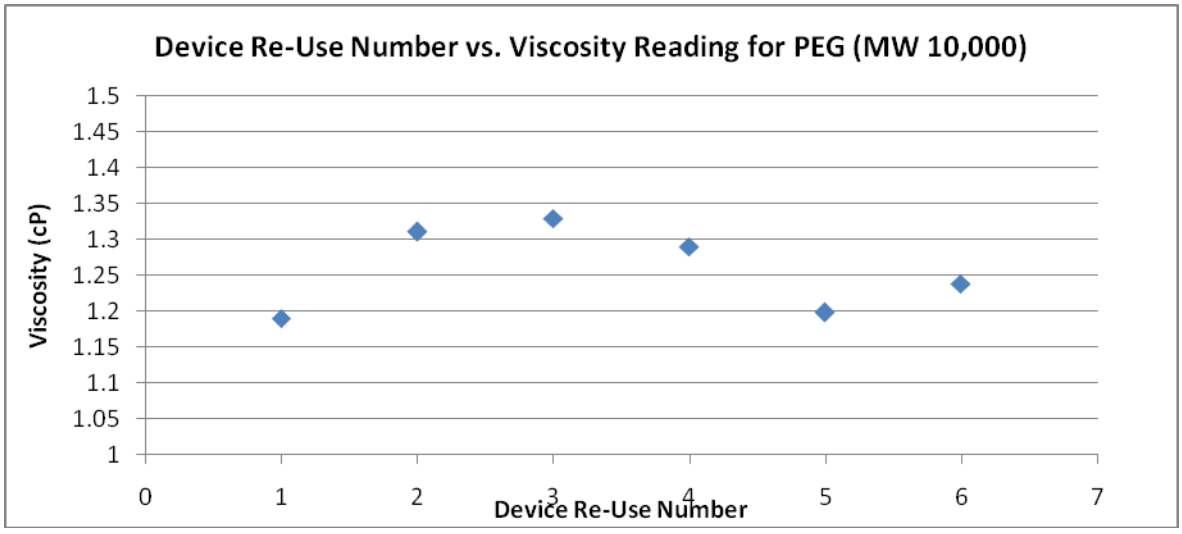

Figure 5-26: *Chart of number time which device is re-used vs. the viscosity reading from the device for the channel-coating ampiphilic polymer polyethylene glycol (MW: 10,000 Da)*

Next, we tested if soaking the channels of the device with PEG 10K might affect viscosity measurements. Devices were soaked for two hours, after which they were dried with air and then re-used. The viscosity of solutions of PEG10K (representing low molecular weight compounds), and HA (representing high molecular weight compounds) were then measured.

A summary of the data for the trials of HA (100 μg/mL) and PEG10K tests in coated and uncoated channels are presented below:

	Polyethylene Glycol 10K (untreated channel)	Hyaluronan (untreated channel)	Polyethylene Glycol 10K (PEG coated channel)	Hyaluronan (PEG coated channel)
Average Viscosity	1.28986	1.38658	1.2899	1.3036
n trials	5	5	6	6
St.Dev:	0.036680622	0.106326441	0.088	0.155435

Table 5-7: *Average viscosity readings and standard deviations for substrates in treated and un-treated channels*

From these trials, it was concluded that device re-use and polymer adsorption did not significantly affect viscosity readings. However, the coatings were shown to have a wetting effect on the PDMS.

Another set of notable observations occurred during the trials of high molecular weight PEO. In these samples of high molecular weight, channel wetting was noted under the following conditions:

Sample	Changes in viscosity post-contact?	Increased hydrophilic behavior
0.3M NaCl	No	No
0.45M K_2SO_4	No	No
PEG 10K	No	Yes
HA in aqueous solution	No	Yes
HA in 0.3M NaCl	No	No
1-5MDa PEO in aqueous solution	No	Yes

1-5MDa PEO in 0.45M K_2SO_4	Yes	Yes

Table 5-8: *Effects of different polymers and different solvents on the surface wetting and measurements of microscale viscometer*

In these observations, ”increased hydrophilic behavior” was defined as the visible “sticking” of very small water droplets to the channel after 10mL air was pushed through the device. A photographic example of this behavior is shown below:

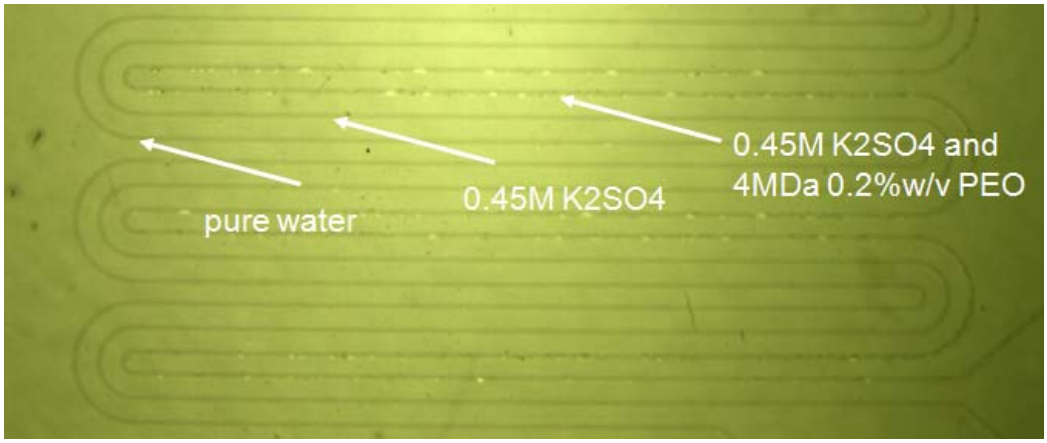

Figure 5- 27: *A device after viscosity measurement of: 4MDa PEO in 0.45M K_2SO_4 salt solution through channel followed by wash and flushing with air*

This picture was taken after a single viscometer trial of 4MDa PEO in 0.45M K_2SO_4 sample under the conditions previously discussed in the viscometer portion of the methods section. This sample was run concurrently with a sample of pure water and 0.45M K_2SO_4. After the viscosity trial, the device was cleaned with approximately 60µL of water, and next about 10mL of air was blown through the device using a syringe. While the air pushed out all of the water in the channels holding water and salt, it left behind a large number of small volume water droplets in the channel, which had held the PEO in salt solution.

We theorize that the PEO in salt solution might be affecting the viscosity measurements through dynamically changing the capillary pressure throughout the length of the viscometers' channels. This question can be addressed in future testing by measuring contact angles of PEO and salt solution within the device at different time points during the viscosity measurement. Differences in these angles at different time points would indicate a change in capillary pressure. Since this seems to only occur for PEO in salt solution, another interesting test would be to see if suspending the 10 kDa PEG polymer in a 0.45M K_2SO_4 solvent would produce the same effects. If it does not, then molecular weight might play a role in the ability of salt to allow PEO to affect viscosity measurements.

These results show that this device is not suitable for re-use for specific polymers in salt solutions. Although most of the data on this topic is currently qualitative, future work can be done on molecular weight dependence and the molecular composition of the polymer. Also, the effects of surface conditions and surface modifications can be investigated to attempt to address these issues.

This section has discussed the theory, evolution, application, and results of a microscale capillary viscometer made from PDMS. Results of trials for low molecular weight controls have shown that the viscometer's measurements are accurate to macro-scale methods. Next this work will discuss the analysis and image acquisition methods use in this system.

CHAPTER 6

IMAGE ACQUISITION AND POST-PROCESSING

Since this method is meant to be a high-throughput process, single process image acquisition method coupled with automated post-processing were desirable qualities for our system. This section discusses the concepts, evolution, and implementation of these methods.

6.1 Image Acquisition

Upon flowing fluid within the channel the refractive index of the fluid/channel interface changed significantly under a diffused transmitted light. Thus by subtracting the initial image of the device it was possible to see only the fluid movement over time to interpret the fluid viscosity.

For these experiments a Stemi SV11 dissecting microscope (Zeiss, Obercochen, Germany) with an attached Motic V3 digital camera (Motic, Xiamen, China) were used to record the fluid movement. One of the biggest challenges in analyzing movies came from these two pieces of hardware. The signal from the Motic camera to the computer experienced random "noisy" changes in illumination intensity. Another contributing factor to this illumination noise was the microscope light source, which was powered by a halogen bulb which had to be changed quite often. Alternative cameras were tried, but could not sufficiently illuminate the entire length of fluid and were not able to provide as large of a field of view as the Motic camera. To prevent changes caused by differences in lighting, settings for software lighting adjustment and tick marks for physical hardware adjustments were made and kept consistent.

The processing of viscosity data was first conducted manually using a commercial image analysis program and was later automated using a program written in Matlab, version 2007b (Mathworks, Natick, MA). The purpose of this customized program is to take in a movie of the fluid travelling within the device under the microscope, and to output the calculated viscosity of the fluid with statistics.

The input to this module was an .avi file of about 10MB in size with an average duration of just over a minute. From this file, the program analyzed the motion in the movie and returns a numerical set of values for the viscosity using the equation derived by Han *et al.*[46] as well as statistical data about the confidence in the derived viscosity.

6.2 First Generation Processing

Since image analysis needs to be able to track the motion of the fluid front over time, the first method chosen was to track the motion of the fluid by eye and track out the fluid's path by hand using ImagePro software (Media Cybernetics, Surrey, British Columbia, Canada). For each frame of the movie, a point was marked manually on the image, and the ImagePro software would calculate the distance between this frame and the subsequent frame. The sum of each of these incremental distances was used to create a single expression for length as a function of time. A screenshot of this method is shown below, where each colored point represents the leading edge of the fluid front in its migration through the viscometer channel. Each color indicates a different fluid stream of the viscometer.

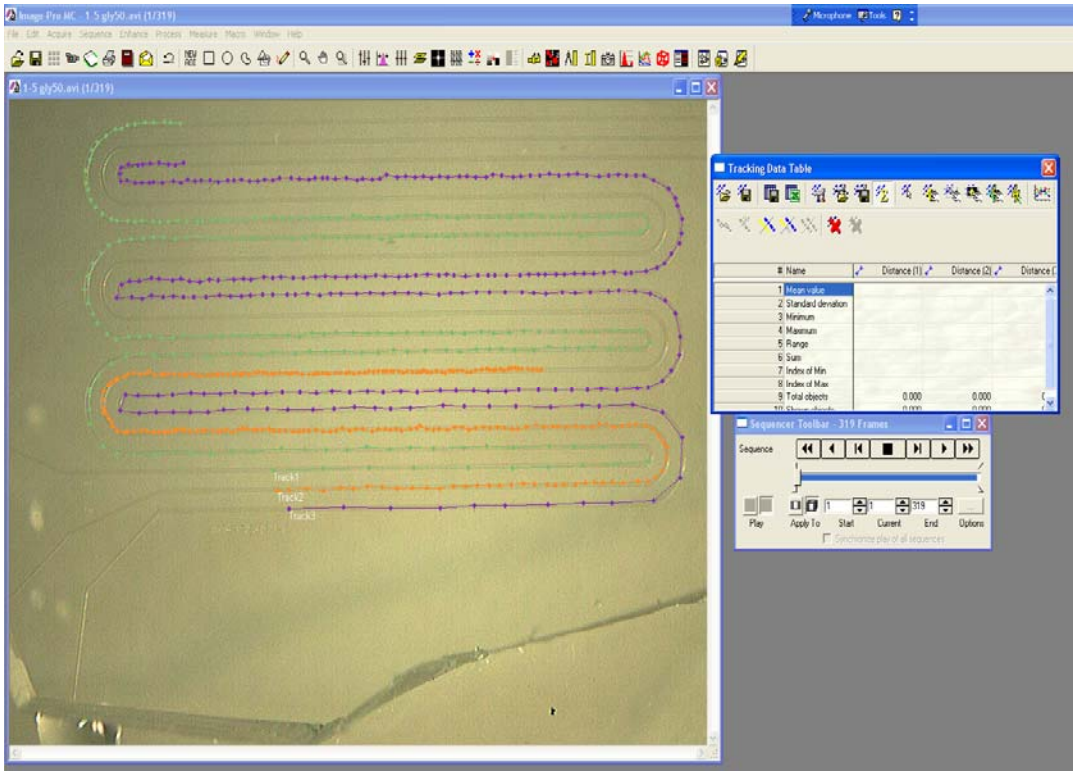

***Figure 6- 28**: ImagePro software screenshot*

Han *et al.* [46] discuss two computational methods for determining viscosity: the first measured speed as a function of time and a second method that monitored only length as a function of time. The practical difference between these two methods is that the first method uses the calculation of a small amount of length change over a small amount of time, while the second measures a large amount of length which is changed a small amount over a small amount of time. This point is significant because it causes the first method to be more error prone at higher frame-rates, while the second method is better for smaller frame-rates.

The first method was also problematic in the early portions of the movie during which the fluid would move around a curve from one frame to the next. In these situations, calculating the absolute distance between the start and endpoints was

insufficient. To account for this error, it was necessary to manually measure out the length of the curved portion and straight portions which the fluid travelled over to accurately assess the total length.

While image analysis using ImagePro was sufficient for early system evaluation and troubleshooting, the method was time consuming and extremely mundane. Thus an alternative automated solution was necessary for analysis.

6.3 Second Generation Automated Processing

Four programs have been written in Matlab for movie analysis: the first to handle input and to compartmentalize data management, the second to convert the movie file format, the third to track the motion of the fluid in each of the three channels, and the fourth movie to calculate viscosity using the equations discussed earlier in this work (code shown in Appendix).

Function Name	***Input***	***Processing***	***Adjustable Parameters***	***Output***
"Findvisc"	Video file name	Passes input string to functions. Clears data from cache after memory intensive processes	None	Viscosity and statistics
"trackprog"	1024x768 color video file	Load movie Filter Subtract background Threshold Resize frames	Start/end frame Background frame	512x384 black and white video file
"stream_label"	512x384 black and white video file	Labels motion of streams over time Conserve pixel noise Convert pixel area over time to length over time Find the R^2 value of the calculated viscosity fit	Off-chip initial lengths	Length as a function of time for each of three channels in device

"calc_stats"	Length as a function of time for each labeled fluid stream	Calculates r^2 statistics and trendline fits for the length as a function of time data	None	Statistics describing viscosity calculation and movie conditions, Calculated viscosity of fluid streams

Table 6-9: *Functions of the viscosity analysis software*

"Findvisc", the first input-handling function, is for handling the data cache due to the memory-intensive nature of the processing in the labeling function, which by itself is sufficient to fill the memory cache.

The second function, "trackprog" first reads the specified file in its native format. The original file format is a 3-channel color 1024x768 movie, but operations on a file of this size are very time consuming. Thus the function takes the green color channel, which for most digital cameras is the channel with the most information and the least noise[56]. The first frame of the movie is then subtracted from each of the subsequent frames. The subtracted movie is then thresholded such that pixels of 1/5 of the maximum intensity to white values. Next all areas of less than 20 pixels in area are discarded, and finally the information is re-written into a more compact integer format of a matrix of 1's and 0's representing the frames of a black and white movie.

The black and white matrix is then passed to the third function, "stream_label", which looks at objects which are contiguous between movie frames. Thus the motion of each stream of fluid can be tracked over time. Each contiguous object is then labeled in the order it is detected (ie. one stream will be composed of pixels represented by 1's, the next of 2's, etc). This can be visualized and recorded as in the screenshot below. The file is then passed to another function which calculated viscosity using the equations discussed in Chapter 3. Finally, the data is written to a reference file which records the

name of the input file, the parameters used in the analysis, and a movie with labeled streams is played back to the user to check for problems in the automation. Below is an example of a labeled frame:

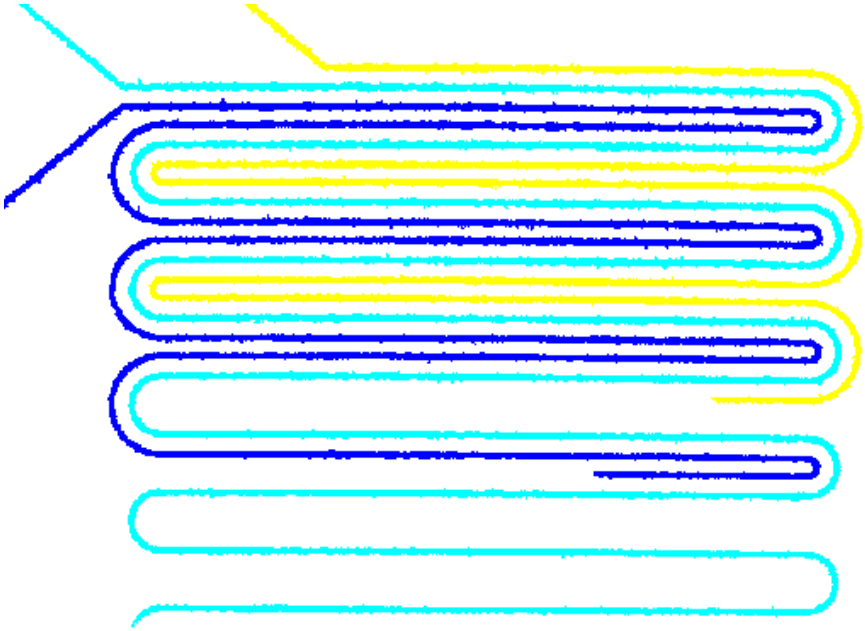

***Figure 6-29**: Labeled streams from stream_label function.*

In the figure above, each color represents a separately labeled fluid stream, with dark blue indicating the stream "1", light blue indicating "2" and yellow indicating "3". Each stream begins to flow from the upper left hand portion of the screen and flows in a serpentine fashion down to the lower left hand corner for a total of 18cm, when recording is terminated. Since the fluids are defined by area, they must be turned into lengths. Lengths are calculated by finding the largest stream area and dividing it by 18cm to determine the cross sectional area, which then is used to determine the length as a function of time for the initial off-screen length of the third stream is added to the length of the growing stream.

After obtaining this matrix of L(t) values for each stream of fluid, the calculation for viscosity according to Han[46] is used by fitting a line to all of the data from his previously referenced equation:

$$\frac{L^2_{reference}(t_2)-L^2_{reference}(t_1)}{t_2-t_1}=\frac{\mu_{sample}}{\mu_{reference}}\frac{L^2_{sample}(t_2)-L^2_{sample}(t_1)}{t_2-t_1}-2d_h^2\frac{P_{capillary,reference}-P_{capillary,sample}}{S\mu_{reference}}$$

A line of formula y = mx+b is then fit to a plot of $\frac{L^2_{reference}(t_2)-L^2_{reference}(t_1)}{t_2-t_1}$ on the y axis vs $\frac{L^2_{sample}(t_2)-L^2_{sample}(t_1)}{t_2-t_1}$ on the x-axis, and the slope of this line is $\frac{\mu_{sample}}{\mu_{reference}}$. The function "stream_label" calculates the R^2 value, which was used to estimate how well the program worked. If the program returned an R^2 value of less than 0.75, the data was discarded as too noisy. An example of the data extracted from the Matlab analysis and plotted manually in excel is given below:

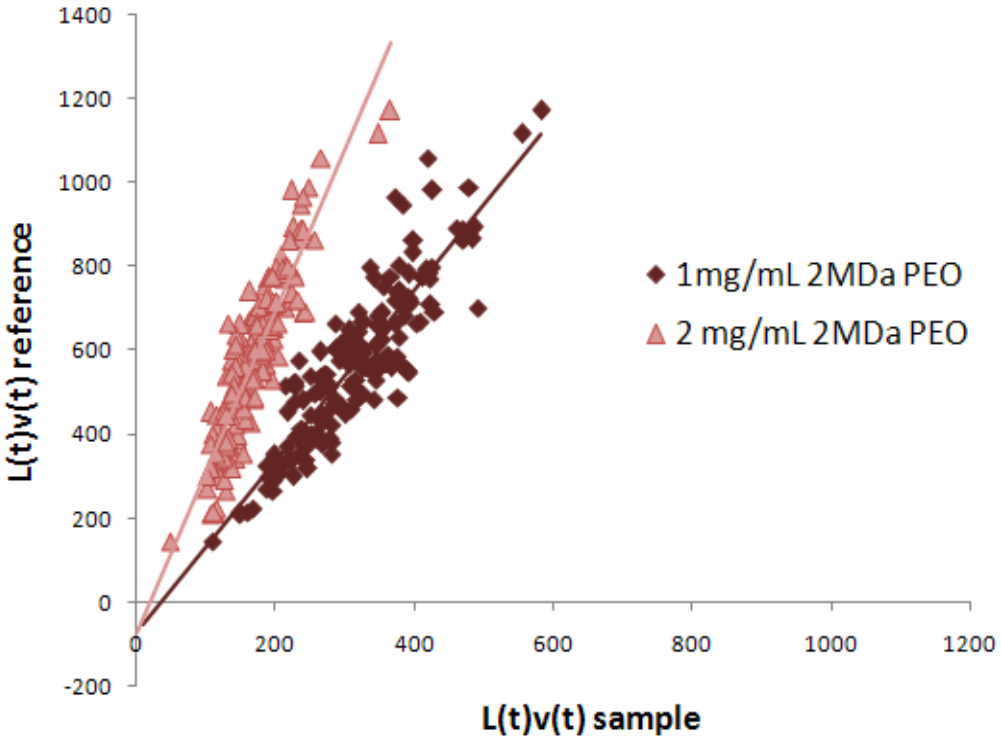

Figure 6-30: *A manual plot of the data processed automatically by Matlab*

The stream_label program also filters out points which are abnormally high for this system by examining the $\frac{L^2(t_2) - L^2(t_1)}{t_2 - t_1}$ values for all three fluids and removing those with values higher than the desired threshold. Abnormally high values for this quantity sometimes occur for a couple frames per movie as a result of noise caused by the lighting or camera recordings.

Finally, relevant data about conditions for analysis and information about the movie file is bundled into a data structure, and saved under the name of the original movie for archiving and organizational purposes.

6.4 Third Generation Automated Processing

The two main problems with the previous second-generation automated image processing were that the hardware used in this project caused non-uniform illumination over each frame of the movies of the fluid over time. This non-uniformity caused the apparent width of the illuminated stream in the movie to fluctuate, introducing errors in the calculations of length over time, which assumed a constant stream width and making recognition of some poorly illuminated portions problematic.

In contrast, the third generation program was based on the use of a template image which allowed the program to equate movie coordinates with pre-determined image coordinates. The program has an image template that is a solid outline of the device with known dimensions. It begins processing each movie by first aligning and resizing itself with the template image. Next, the threshold was lowered to enhance recognition of poorly illuminated portions of the screen, and the points which corresponded to both the template and the movie were accepted as part of the screen.

Thus the use of the template prevented low illumination problems by allowing the threshold to be lowered without introducing errors from pixel overlap between streams.

However, due to time constraints this program was not adequately tested and optimized, thus results and code from the program are not published herein, and the data analysis was instead performed by the functions discussed in 6.2.

This chapter has described the specifics of the method for determining an unknown polymer molecular weight from an unknown concentration of dilute polymer solution using fluid viscosity. It has also described the use of a modular system to determine viscosity of a fluid. Next the efficacy of this method and the devices shall be discussed.

CHAPTER 7

METHOD APPLICATION

This section first discusses the application of the proposed method to the characterization of the synthetic polymer PEO and our preliminary work on characterization of the biopolymer HA.

7.1 Polyethylene Oxide Characterization

Here we will show the results for the characterization of the molecular weight of PEO using our method. The system will be used to estimate the hydrodynamic volume of a single PEO molecule and will then evaluate the effect of two different solvents on this hydrodynamic volume.

Four molecular weight standards of nominal molecular weight 1, 2, 4 and 5MDa were purchased from Sigma. These standards were then dissolved in water at 3-4 concentrations under the solvent conditions of 0M K_2SO_4 and 0.45M K_2SO_4. These two conditions were chosen due to pre-existing information on K and a constants describing solvent effects from Bailey *et al.* [19].

First, the microscale system was used to evaluate the solvent condition of 0M K_2SO_4. The results are shown below.

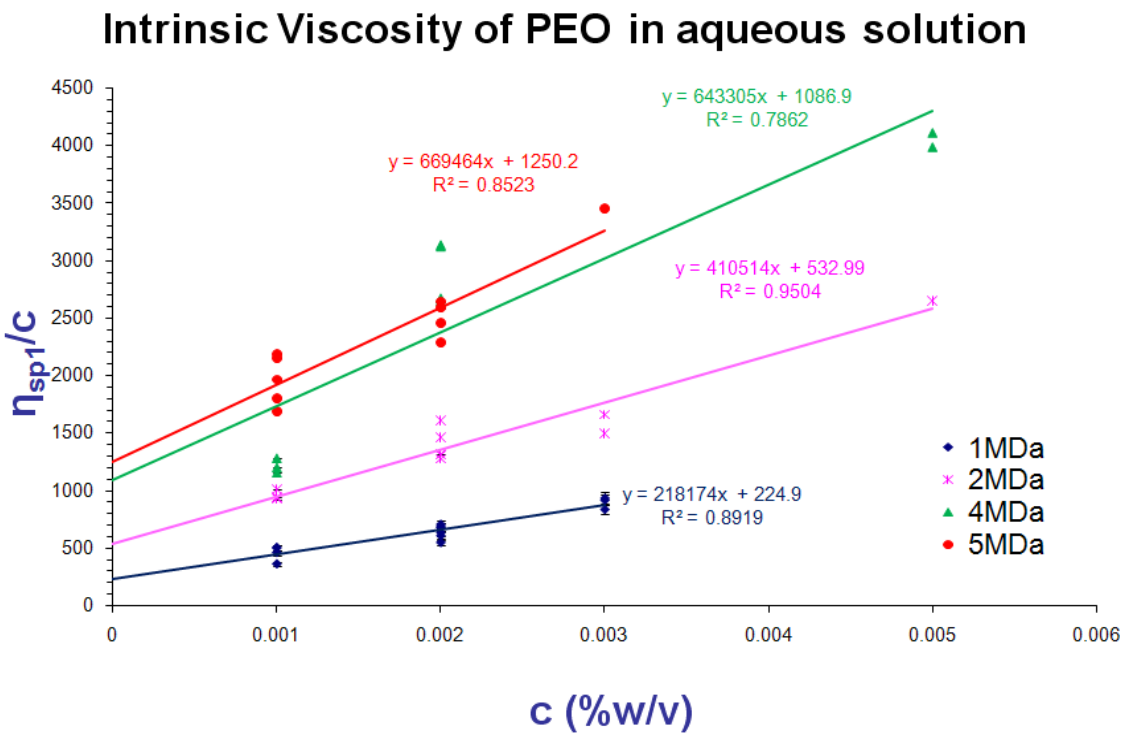

Figure 7-31: *Chart of concentration vs specific viscosity over concentration used to find extrapolated values for intrinsic viscosity [η] in solvent1 (0M K_2SO_4)*

This plot of concentration vs. specific viscosity divided by concentration is used to show the relationship of the bulk solution viscosity to the concentration of polymer in the solution. The Huggins equation discussed earlier (and shown again below) can be used to estimate hydrodynamic volume by extrapolating the function of each molecular weight standard to zero.

$$\frac{\eta_{sp}}{c} = [\eta] + k'[\eta]^2 c \qquad (2\text{-}19)$$

Thus each of the lines shown in the intrinsic viscosity chart above, the y-intercept of each fit line represents an intrinsic viscosity measurement.

Next, the K and a constants can be derived by charting out a series of [η] values vs. the known molecular weights in a log-log plot. This relationship is derived from the Mark-Houwink equation (shown below).

$$[\eta] = K\overline{M}_v^{\,a} \tag{2-10}$$

$$\log[\eta] = \log(K) + a(\log \overline{M}_v) \tag{7- 29}$$

Thus since the experiment was provided with four different molecular weight standards for testing, four points were obtained for the chart. It can be seen from the equation above that the slope of the resultant graph yields the a constant, while the y-intercept of the graph indicates the exponential value of K. This chart is shown below:

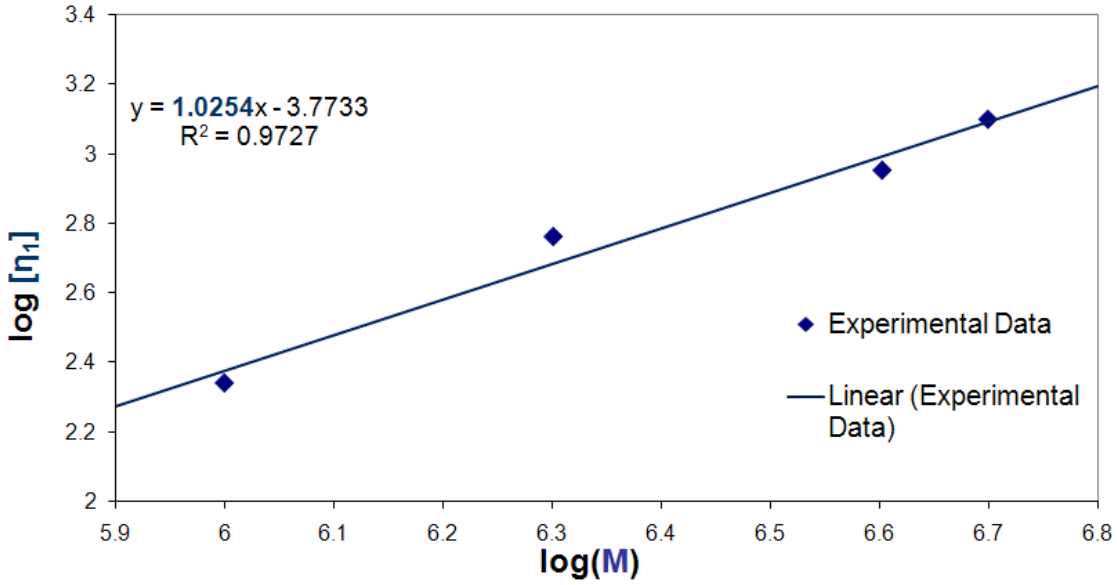

Figure 7-32: *Experimentally determined K and a constants from log intrinsic viscosity vs. molecular weight*

Next the "solvent 2" condition of 0.45M K_2SO_4 was applied. It should be noted that at this higher salt concentration, precipitation of salt and polymer was a significant

problem for all concentrations above 0.1%w/v, a concentration which is well below the limit previously indicated for dilute viscometry (~0.5%w/v).

Results for this solvent condition were obtained using a macroscale Ubbelohde viscometer. Due to resource and time constraints, this test was run for only three different molecular weights (1,2,5 MDa). Concentration and specific viscosity were plotted as previously discussed under solvent condition 1 and are shown below:

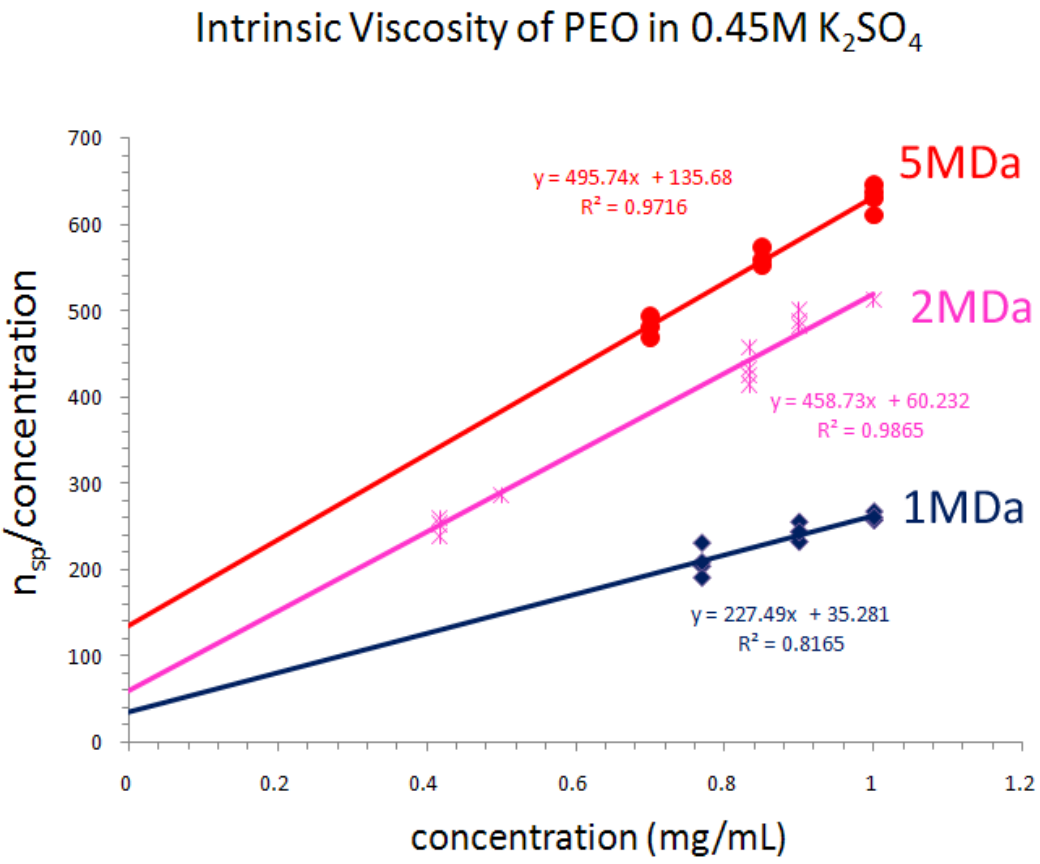

Figure 7-33: *Chart of concentration vs. specific viscosity over concentration used to find extrapolated values for intrinsic viscosity [η] in solvent2 (0.45M K_2SO_4)*

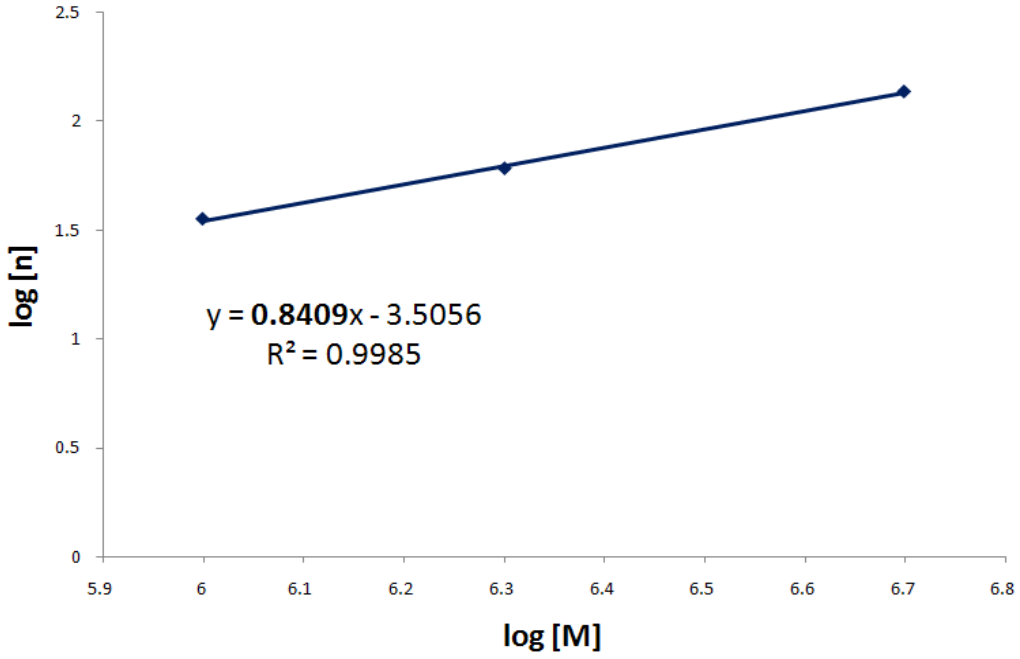

Figure 7-34: *Experimentally determined K and a constants from log hydrodynamic diameter vs. molecular weight*

As discussed for the previous solvent condition, these charts can then be used to solve values for *K* and a for this solvent2 condition of 0.45M K_2SO_4. The results from the viscosity studies under these two solvent conditions can be summarized as follows:

	This Work	**Bailey 1976**
a1 (0M K_2SO_4)	1.024	0.76
K1 (0M K_2SO_4) $\frac{cm^3}{g}(\frac{g}{mol})^{-a}$	0.000169	0.012
a2 (0.45M K_2SO_4)	0.84	0.5
K2 (0.45M K_2SO_4) $\frac{cm^3}{g}(\frac{g}{mol})^{-a}$	0.00031	0.13

Figure 7-35: *Experimental vs. theoretical values for PEO in two solvents*

Examination of the values for *K* and a values shows the expected trend in our data. In solutions with higher salt concentrations, the hydrodynamic volume is contracted due to the suppression of intramolecular repulsive forces, and solutions of lower salt concentrations the volume is predictably increased.

Despite the correct trend, the numerical literature values for *K* and *a* are different. Reasons for this might be due to different sources of PEO, and the lack of formal evaluation of our samples' molecular weights.

To attempt to address the latter problem, Gel Permeation Chromatography (GPC) analysis was used to obtain the Mw, Mn, and the Polydispersity index. This provides an estimate for the range of Mv, which is less than the weight averaged molecular weight and greater than the number averaged molecular weight.

With this set of experimentally determined *K* and *a* constants, one can construct a set of standard curves describing the behavior of PEO in solutions of different molecular weights in different solvents conditions.

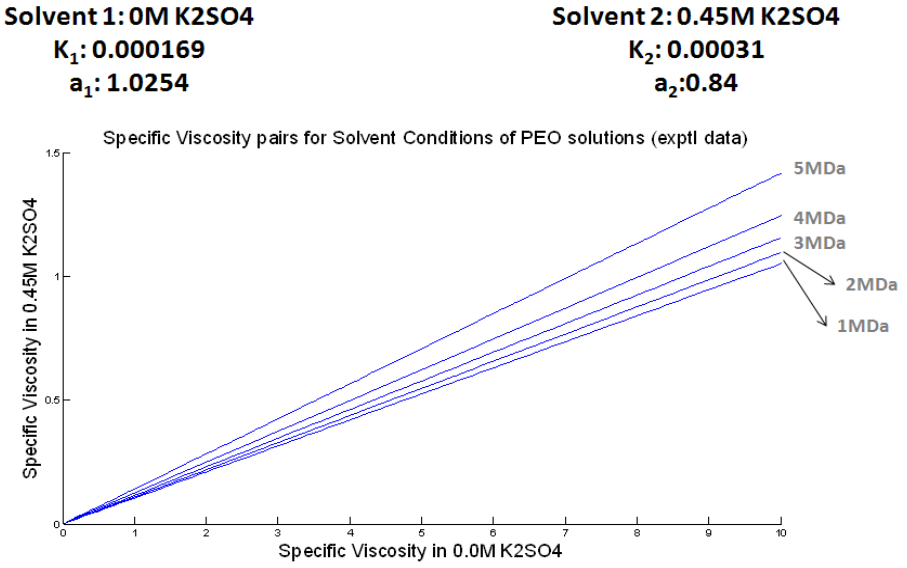

Figure 7-36: *Constructed standard curve for PEO in two solvent conditions for molecular weights of 1-5MDa*

However, the actual agreement of our data with this curve has shown to be poor. For instance, the specific viscosity of 0.1% of 1MDa PEO is 1.9, but in 0.45M K2SO4 it is 0.5. This figure is quite a big higher than the estimates found using the graph, This is most likely due to the small number (n=3) of molecular weight standards. Increasing the number of standards used for the curve would raise the accuracy of these measurements

7.2 Hyaluronic Acid (HA)

This section shows preliminary results of the application of our method to HA. However, due to the prohibitively high cost of HA standards (~$500/10mg), our method was not fully evaluated for this polymer. Instead, in this section we will first show that the viscosities measured in this work are comparable to values calculated from constants in literature. Next, we will show that the sensitivity of our method is (1) sufficient for measuring viscous changes in HA solutions due to solvent, and (2) that different molecular weights of HA show measurably different viscous behavior for known concentrations of polymer.

Four samples of HA were used in this study--two purchased from Sigma, and two obtained from the Chen Lab's fermentation products. The two fermentation product samples were derived from genetically modified E. coli and provided by Dr. Hyun-Dong Shin (Chen Lab, Georgia Institute of Technology - Department Chemical and Biomolecular Engineering) for his studies of microbial hyaluronan production at 24 and 40 hours. The two Sigma samples have putative molecular weights of 1.667 MDa, as measured using GPC by Dr. Zichao Mao (Chen Lab) and 0.75-1.3MDa ([17, 57])

Next, these solvent conditions were applied to varying concentrations HA and the results were compared to those in literature that were conducted using macroscale methods.

1.67 MDa HA polymer in 0.3M NaCl			
Concentration (ug/mL)	**η_{sp}**	**η_{sp} from literature**	**% Error from literature**
250	1.5728	1.6145	2.58%
200	1.4048	1.475	4.76%
150	1.289	1.344	4.09%
75	1.209	1.162	4.04%
50	1.1139	1.106	0.71%

Table 7-10: *Comparison of extrapolated literature values with experimental values for specific viscosity of various HA dilute polymer solutions in 0.3M NaCl*

These evaluations were performed on solutions of HA and NaCl purchased from Sigma-Aldrich. Values for η_{sp} literature were obtained using the *K* and a constants determined by Fouissac *et al.* [58] in the Huggins Equation for the set of concentrations used in this experiment. These calculated values showed a percentage absolute error from the experimentally determined viscosities by less than five percent. However, it should be mentioned that although the behavior of the polymer seems to agree with these literature values, it is uncertain how closely our sample from Sigma corresponds to the literature reference's source of HA. Thus we note that this correspondence to literature values could be incidental.

For HA, we chose solvent conditions of water (0M NaCl) and 0.3M NaCl. The first condition of 0M NaCl was chosen because samples showed good resolution between different concentrations, making the determination of an intrinsic viscosity less error-prone. The second condition of 0.3M NaCl was chosen for the good agreement between our preliminary experimental results and extrapolated theoretical viscosity results from

literature. Due to difficulties in determining the actual molecular weight of the fermentation samples, only the two Sigma samples of HA were used for analysis. The flat nature of the plot of 680KDa is likely due to errors in the calculated concentrations of product, and will require further testing.

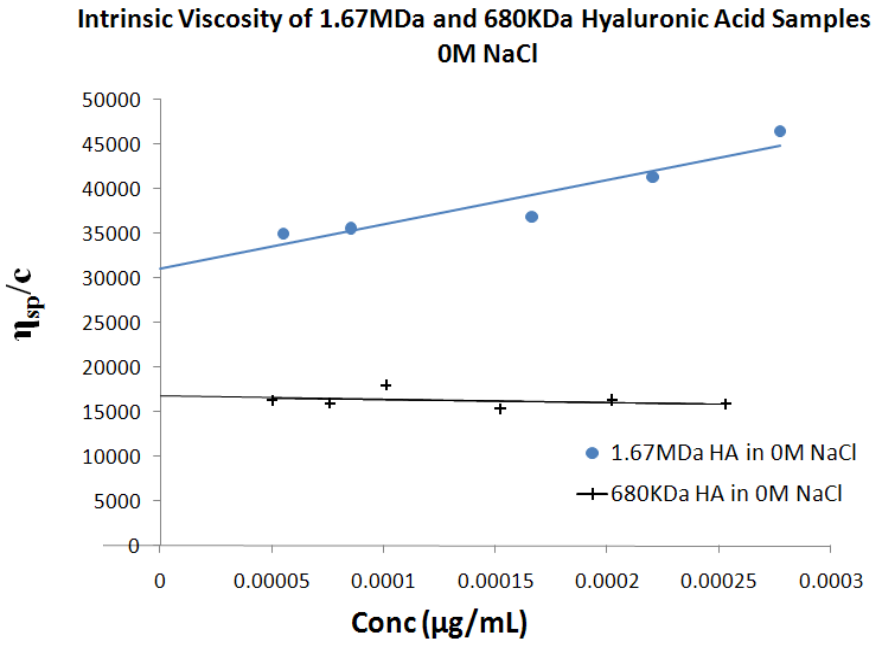

Figure 7- 37: *Concentration vs. specific viscosity over concentration used to find extrapolated values for intrinsic viscosity [η] in solvent2 (0M NaCl)*

Next, from the Mark-Houwink equation , shown again below for convenience, it can be seen that for one solvent condition, at least two "points" representing a molecular weight and a corresponding intrinsic viscosity are necessary to designate the *a* and *K* values to fit the line. Increased specificity could be easily applied to this process by increasing the amount of characterized samples to determine these constants.

$$[\eta] = K\overline{M}_v^{\,a} \qquad (2\text{-}10)$$

Currently, two important observations have been made supporting the viability of this method.

First, for a given HA sample with a known molecular weight of 1.67MDa, it is apparent that in different salt conditions of the solvent, the solution undergoes dramatic and noticeable alterations in viscosity. This is evident from the plot below, which charts the changes in the viscosity/concentration relationship with increasing salt concentration:

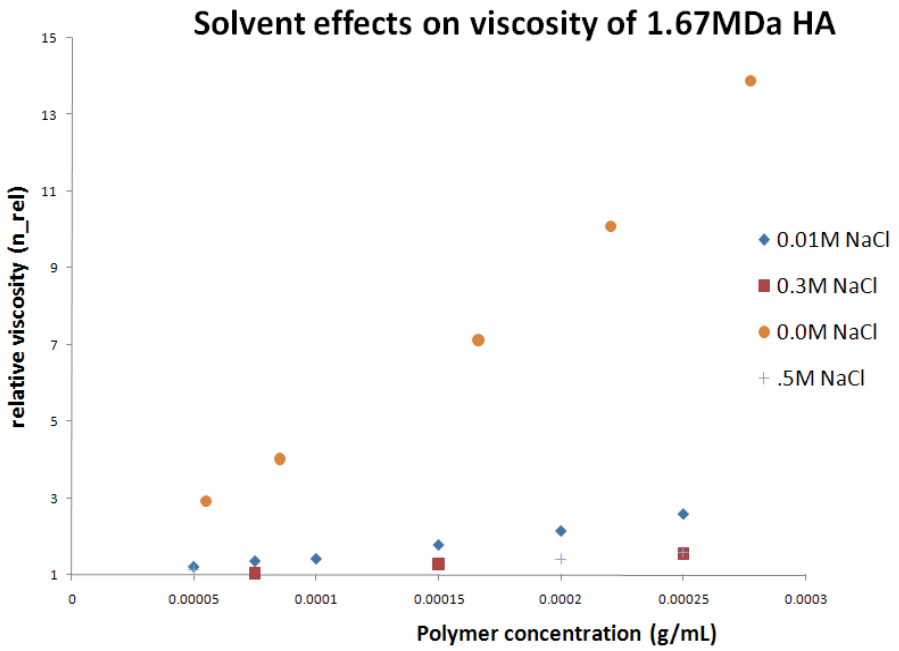

Figure 7-38: *Effects of solvent salt on HA viscosity.*

This finding corresponds with previous findings in literature that document the decrease in viscosity due to an increase in solution salt concentrations (see Chapter 2 for references).

The second key finding was that solutions with the same salt concentration but different molecular weights of polymer solutions show noticeable differences in viscosity. These results are shown below.

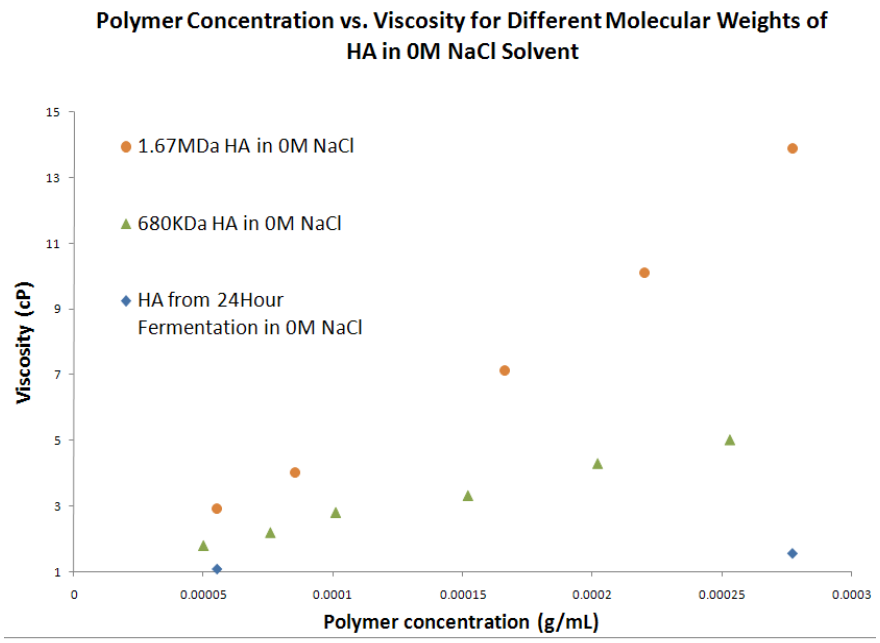

Figure 7-39: *Effects of differences in molecular weight on solution viscosity.*

As seen above, different molecular weights of HA show clear differences in viscosity over known concentrations. The fermentation sample appears to be of molecular weight below 680kDa. However, this result could be due to the influence of the lyophilization process used to purify and re-suspend the sample, and will need verification testing and more trials for further investigation.

Thus although our method has not yet been validated, this method appears to show potential for our ultimate goal of predicting molecular weight from observations of salt-induced changes in molecular conformation.

The intended goal of this system and its method is not to replace more expensive, high precision methods and equipment, but rather to provide a high-throughput and low-cost alternative capable of examining changes in a system over time to obtain an estimate of molecular weight as a function of fermentation or synthesis conditions. Thus, it

should not be expected to make extremely accurate molecular measurements. We were able to obtain uncharacterized microbial fermentation time-points products for analysis in this work, giving us an opportunity to apply our method and also to evaluate the method's experimental results using traditional methods

First, for samples of HA, specific viscosity measurements of known concentrations do indicate relative molecular weight. Second, samples of HA in solvents of higher salt concentrations show a significant decrease in viscosity when compared to their viscosity in lower salt concentrations. However, these results cannot be used as present to determine molecular weight, since their own molecular weights have yet to be determined by GPC [17, 57]. Calculations of the intrinsic viscosities of the two commercial HA samples has been shown in 0M H_2O.

In summary, we have shown the preliminary testing of a method to determining molecular weight on PEO and begun assessment of its use on HA. We have used our analysis system to evaluate the intrinsic viscosity of different molecular weights of PEO and to describe the behavior of these different molecular weights according to two different solvent conditions. In HA, we have shown that this method shows promise for determining HA molecular weight since its viscosity varies notably in the tested solvent conditions, and nominal molecular weights of known concentration do show differences in viscosity.

CHAPTER 8

CONCLUSION

This section will review and discuss the contribution, applications, and possible further development of this work. First it will discuss our application of the method to PEO and next the preliminary results of our application of the method to HA.

8.1 Contribution of Thesis

Although there are a number of current methods for characterizing polymeric molecular weight, none of these current methods are designed for the application of characterizing the molecular weight of small, dilute polymer solutions of unknown concentrations. This is an important application for the field of polymer science, where the analysis of polymer production, whether in microbes, via metabolic engineering, or by chemical synthesis, is important for monitoring changes in molecular weight over time. Current methods in molecular weight characterization are unable to address this need because they require concentration to be known ahead of time. Additionally, many methods require long sample analysis and preparation times, high sample concentrations and large sample volumes. In addition, they require costly instruments.

Compared to conventional techniques, methods in this thesis have significant advantages. First, our microscale method can find fluid viscosity in approximately half the time as a macroscale viscometer. Second, the volume and concentration of required sample are small. All modules of the microscale molecular weight determination system required only dilute concentrations between 50-300 μg/mL for HA studies and 100-500 μg/mL for PEO studies. These concentrations are comparable to the low end of

concentrations in conventional techniques. However, because the volume required for microscale analysis is much smaller, the overall amount of polymer required for the analysis is also small. Lastly, the cost per assay for the micro system is relatively low. The chips themselves are ~10 cents each, and additional requirements would be a simple microscope and camera system, which present one-time costs. The advantages of our method as compared with other current methods are shown in the table below:

Method	Cost	Speed	Total Polymer Required	Solution Volume Required
Gel Permeation Chromatography *(GPC)*	$\$10^5$	hours	10^{-3}g	10^{-3}L
Macroscale Viscometry	$\$10^2$	hours	10^{-3}g	10^{-3}L
Microscale Analysis	**$\$10^2$**	**minutes**	**10^{-6}L**	**10^{-6}L**

Table 8-11: *Comparison of microscale method proposed in this work to previous methods*

Although the efficacy of the system as a whole for the evaluation of molecular weight has not yet been fully demonstrate, the technique has potential in reducing the cost and time for assessing molecular weights and concentrations of polymers in solution.

8.2 Future Work

Although this work has presented results for some applications of the microscale analysis system, there are areas where significant progress can be made. This includes the integration of on-chip viscosity measurement and dialysis, increasing the sensitivity of the measurements, microscale verification of the macroscale PEO tests, and application of the testing methods to HA.

First, the polymer output from the dialysis process should be applied to the viscometer system to prove the validity of using the two in an integrated system. A scheme for monolithic evaluation of the two devices should also be evaluated.

Second, measurement sensitivity can also be improved. Since our method is based on the use of experimental data represented on a standard curve, increasing the sensitivity of the viscosity measurements should increase the precision of our method. One way is to improve the software post-processing algorithm to employ template matching and smoothing for better image analysis and quantification. Other ways in which sensitivity might be improved include optimizing the frame-rate of the movies recorded to attempt to obtain more length over time data. Consistent illumination schemes can also be used to improve viscosity measurements.

Third, the effects of a changing capillary pressure should also be examined to ensure that viscosity readings are consistent over trials. Future research can begin to address this issue by investigating changes in contact angle of PEO in the 0.45M K_2SO_4 solvent condition over time during the assay.

Another aspect of this work which would present a vast improvement over current methods would be the addition of another microscale device which would be able to create serial dilutions of polymer solution. This would obviate the need for the tedious and time-consuming process of making serial dilutions of small amounts of polymer and solvent when analyzing the polymer standards to obtain K and a constants. It would also make it easier to create dilutions of polymer solutions so that many different pairs of solvent viscosities can be measured, thus improving measurements for molecular weight. Also the preparation of these solutions is a wasteful process since they must be mixed at

volumes large enough to measure using a laboratory balance with a sensitivity range of about 5mg.

8.3 Potential Applications Using Techniques Developed in This Work

Ideally this method would be applied to the commercial production of a number of different polymers, both synthetic and biologically derived. Metabolic Engineering's recent successes in the increased production of a number of commercially important molecules has created a great need for the ability to characterize small dilute titers of polymers, and we hope that this method will be instrumental in helping to fulfill this need.

The efficacy of the micro-scale dialysis module alone provides a significant step forward for polymer purification, which is currently a long process requiring the need for a number of manual steps including encasing solutions for dialysis, changing dialysis fluid, lyophilizing the dialyzed samples, and re-suspending the samples in the correct solvent. We hope that this microscale method provides an improvement over this labor-intensive macroscale method.

The synthesis of a polymer molecule, especially within a biological organism such as a microbe, is a complex process which can be affected by a number of factors [18, 59-61]. By reducing the volume and concentration of samples involved in examining the product of these processes, we can assay a number of conditions affecting polymer synthesis in a high-throughput manner. Some possible applications for examining the synthesis of synthetic polymers include the high throughput assaying of different concentrations and species of catalyst compounds.

The conceptual development of this microscale molecular weight analysis method is also significant for basic biological research. For biologically derived polymers there exists a huge array of assayable conditions including concentrations of feedstock, composition of feedstock, time-sensitive growth, oxygen concentration, and genetic modification of metabolic pathways, to name a few [18]. Varying these conditions and using the molecular weight of biopolymer as an output can tell us quite a bit about the way that the cell regulates the use of its resources. Thus it is clear that this method is of great value to the progress of scientific research in a number of different fields.

This chapter has described the general contribution of this work to address the need for a low cost, high throughput method to characterize small dilute volumes of unknown concentration and unknown molecular weight.

This work has also shown a great potential for future growth. Here I have discussed ways in which the method presented may be improved, including adding more hardware modules to the system, extending the application of this method to other types of polymers to prove its applications to polymer synthesis, and conducting a complete run through of the integrated system. This work lays a solid foundation for the method which I hope will be built upon by future scientists and engineers.

Finally, applications for the findings from the work in basic science and industrial uses have been presented. Since this device was intended to be used to conduct metabolic engineering studies, I believe that it will greatly benefit basic biological studies of metabolic pathways and the production of complex molecules within whole cells. Since viscometry is a well developed area of study which is already used in research, I

also hope that this work will have immediate applications for more traditional methods of synthetic polymer production.

REFERENCES

1. Rudin, A., *The Elements of Polymer Science and Engineering*. Second ed. 1999.
2. Lapcik, L., et al., *Hyaluronan: Preparation, structure, properties, and applications.* Chemical Reviews, 1998. **98**(8): p. 2663-2684.
3. Young, RJ, .Lovell, PA, *Introduction to Polymers, Second Edition*. Second ed. 1991: Nelson Thornes.
4. Garg, H., Hales, Charles A. *Chemistry and Biology of Hyaluronan*. 1st ed. 2004, Boston: Elsevier.
5. Ramakrishna, S., et al., *Biomedical Applications of Polymer-Composite Materials: a Review.* Composites Science and Technology, 2001. **61**(9): p. 1189-1224.
6. Bailey, F., Powell, G. M., Smith, K. L., *HIGH MOLECULAR WEIGHT POLYMERS OF ETHYLENE OXIDE - SOLUTION PROPERTIES.* Industrial and Engineering Chemistry, 1958. **50**(1): p. 8-11.
7. *"Microbial Cell Factories: About".* 2006 http://www.microbialcellfactories.com/info/about/.
8. Keasling, J.D., *Synthetic Biology for Synthetic Chemistry.* ACS Chemical Biology, 2008. **3**(1): p. 64-76.
9. Yu, H., Stephanopoulos G., *Metabolic engineering of Escherichia coli for biosynthesis of hyaluronic acid.* Metabolic Engineering, 2008(10): p. 24-32.
10. Cowman, M.K. and S. Matsuoka, *Experimental approaches to hyaluronan structure.* Carbohydr Res, 2005. **340**(5): p. 791-809.
11. Thorsen, T., S.J. Maerkl, and S.R. Quake, *Microfluidic large-scale integration.* Science, 2002. **298**(5593): p. 580-584.
12. Whitesides, G.M., *The origins and the future of microfluidics.* Nature, 2006. **442**(7101): p. 368-373.
13. Eyal, S. and S.R. Quake, *Velocity-independent microfluidic flow cytometry.* Electrophoresis, 2002. **23**(16): p. 2653-7.
14. Khandurina, J., et al., *Integrated system for rapid PCR-based DNA analysis in microfluidic devices.* Analytical Chemistry, 2000. **72**(13): p. 2995-3000.
15. Liao, Y.H., et al., *Hyaluronan: Pharmaceutical characterization and drug delivery.* Drug Delivery, 2005. **12**(6): p. 327-342.
16. Shih, C., *Methods for HA grafting to microbeads*.
17. Shiedlin, A., et al., *Evaluation of hyaluronan from different sources: Streptococcus zooepidemicus, rooster comb, bovine vitreous, and human umbilical cord.* Biomacromolecules, 2004. **5**(6): p. 2122-2127.
18. Mao, Z. and R.R. Chen, *Recombinant synthesis of hyaluronan by Agrobacterium sp.* Biotechnol Prog, 2007. **23**(5): p. 1038-42.
19. Bailey, F., Koleske, J., *Poly(ethylene oxide)*. First ed. 1976: Academic Press.
20. Alkox, C. (2007) *ALKOX - What is Alkox?*
21. Briscoe, B., P. Luckham, and S. Zhu, *Rheological study of poly(ethylene oxide) in aqueous salt solutions at high temperature and pressure.* Macromolecules, 1996. **29**(19): p. 6208-6211.
22. Pasut, G. and F.M. Veronese, *Polymer-drug conjugation, recent achievements and general strategies.* Progress in Polymer Science, 2007. **32**(8-9): p. 933-961.

23. Dimitrov, P., et al., *High molecular weight functionalized poly(ethylene oxide).* Polymer, 2002. **43**(25): p. 7171-7178.
24. Huang, J.L., H.Y. Wang, and X.Y. Tian, *Preparation of PEO with amine and sulfadiazine end groups by anion ring-opening polymerization of ethylene oxide.* Journal of Polymer Science Part a-Polymer Chemistry, 1996. **34**(10): p. 1933-1940.
25. Yokoyama, M., et al., *Synthesis of Poly(Ethylene Oxide) with Heterobifunctional Reactive Groups at Its Terminals by an Anionic Initiator.* Bioconjugate Chemistry, 1992. **3**(4): p. 275-276.
26. Atkins, P.W., *Physical Chemistry, Sixth Edition*. Sixth ed. 1998: Oxford University Press.
27. Volkov, A.V., et al., *Effect of Copper Ions on Phase State in Polymer Blend-Based on Poly(Vinyl Alcohol) and Poly(Acrylic Acid).* Vysokomolekulyarnye Soedineniya Seriya a & Seriya B, 1993. **35**(2): p. B70-B75.
28. Lee, H.G. and M.K. Cowman, *An agarose gel electrophoretic method for analysis of hyaluronan molecular weight distribution.* Anal Biochem, 1994. **219**(2): p. 278-87.
29. Huggins, M.L., *Molecular weights of high polymers.* Industrial and Engineering Chemistry, 1943. **35**: p. 980-986.
30. Huggins, M.L., *The viscosity of dilute solutions of long-chain molecules V Dependence on the solvent.* Journal of Applied Physics, 1943. **14**(5): p. 246-248.
31. Huggins, M.L., *The viscosity of dilute solutions of long-chain molecules III the Staudinger viscosity law.* Journal of Applied Physics, 1939. **10**(10): p. 700-704.
32. Huggins, M.L., *The viscosity of dilute solutions of long-chain molecules. IV. Dependence on concentration.* Journal of the American Chemical Society, 1942. **64**: p. 2716-2718.
33. Sigma-Aldrich, *Inquiry regarding molecular weights of Hyaluronan and PEO samples*, S. Chemicals, Editor. 2008.
34. Bird, E., Stewart, B., and W. Lightfoot. *Transport Phenomena*. Second ed. 2002: Wiley and Sons.
35. Weigl, B.H., et al., *Whole blood diagnostics in standard gravity and microgravity by use of microfluidic structures (T-sensors).* Mikrochimica Acta, 1999. **131**(1-2): p. 75-83.
36. Weigl, B.H. and P. Yager, *Microfluidics - Microfluidic diffusion-based separation and detection.* Science, 1999. **283**(5400): p. 346-347.
37. Weigl, B.H. and P. Yager, *Silicon-microfabricated diffusion-based optical chemical sensor.* Sensors and Actuators B-Chemical, 1997. **39**(1-3): p. 452-457.
38. Yager, P., et al., *Microfluidic diagnostic technologies for global public health.* Nature, 2006. **442**(7101): p. 412-418.
39. Weigl, B.H., et al., *Lab-on-a-chip sample preparation using laminar fluid diffusion interfaces - computational fluid dynamics model results and fluidic verification experiments.* Fresenius Journal of Analytical Chemistry, 2001. **371**(2): p. 97-105.
40. Giancoli, D.C., *Physics for Scientists and Engineers (3rd Edition)*. Third ed. 2000: Prentice Hall.

41. Web, I.T.P. *Viscosity Number ISO - 137*. 2008 [cited 2008 5/16/2008]; Available from: www.ides.com/property_descriptions/ISO307.asp.
42. Srivastava, N. and M.A. Burns, *Analysis of non-Newtonian liquids using a microfluidic capillary viscometer.* Analytical Chemistry, 2006. **78**(5): p. 1690-1696.
43. Srivastava, N. and M.A. Burns, *Microfluidic pressure sensing using trapped air compression.* Lab on a Chip, 2007. **7**(5): p. 633-637.
44. Srivastava, N., R.D. Davenport, and M.A. Burns, *Nanoliter viscometer for analyzing blood plasma and other liquid samples.* Anal Chem, 2005. **77**(2): p. 383-392.
45. van der Heyden, F.H.J., et al., *A low hydraulic capacitance pressure sensor for integration with a micro viscosity detector.* Sensors and Actuators B-Chemical, 2003. **92**(1-2): p. 102-109.
46. Han, Z., X. Tang, and B. Zheng, *A PDMS viscometer for microliter Newtonian fluid.* Journal of Micromechanics and Microengineering, 2007. **17**(9): p. 1828-1834.
47. Guillot, P., et al., *Viscosimeter on a microfluidic chip.* Langmuir, 2006. **22**(14): p. 6438-6445.
48. Choi, *PEG modified PDMS for protein and cell resistant surfaces in microbioreactor. I*n *conference*. 2003.
49. Ebara, M., et al., *Surface modification of microfluidic channels by UV-mediated graft polymerization of non-fouling and 'smart' polymers.* Radiation Physics and Chemistry, 2007. **76**(8-9): p. 1409-1413.
50. Huh, C. and S.G. Mason, *Steady Movement of a Liquid Meniscus in a Capillary Tube.* Journal of Fluid Mechanics, 1977. **81**(Jul13): p. 401-419.
51. Duffy, D.C., et al., *Rapid prototyping of microfluidic systems in poly(dimethylsiloxane).* Analytical Chemistry, 1998. **70**(23): p. 4974-4984.
52. Sia, S.K. and G.M. Whitesides, *Microfluidic devices fabricated in poly(dimethylsiloxane) for biological studies.* Electrophoresis, 2003. **24**(21): p. 3563-3576.
53. Bowden, N., et al., *The controlled formation of ordered, sinusoidal structures by plasma oxidation of an elastomeric polymer.* Applied Physics Letters, 1999. **75**(17): p. 2557-2559.
54. Company, T.D.C., *Viscosity of Aqueous Glycerine Solutions* http___www.dow.com_PublishedLiterature_dh_0032_0901b803800322bd.pdf_filepath=glycerine_pdfs_noreg_115-00678, Editor. 2008, Dow Chemical Company.
55. Kirincic, S. and C. Klofutar, *Viscosity of aqueous solutions of poly(ethylene glycol)s at 298.15 K.* Fluid Phase Equilibria, 1999. **155**(2): p. 311-325.
56. McHugh, S.T. *Digital Camera Sensors*. Color Photography Tutorials 2005-2008 [cited 2008; Available from: http://www.cambridgeincolour.com/tutorials/camera-sensors.htm.
57. Beeson, J.G., et al., *Adhesion of Plasmodium falciparum-infected erythrocytes to hyaluronic acid in placental malaria.* Nature Medicine, 2000. **6**(1): p. 86-90.
58. Fouissac, E., et al., *Influence of the Ionic-Strength on the Dimensions of Sodium Hyaluronate.* Macromolecules, 1992. **25**(21): p. 5613-5617.

59. Widner, B., et al., *Hyaluronic acid production in Bacillus subtilis.* Appl Environ Microbiol, 2005. **71**(7): p. 3747-52.
60. Armstrong, D.C. and M.R. Johns, *Culture conditions affect the molecular weight properties of hyaluronic acid produced by Streptococcus zooepidemicus.* Applied and Environmental Microbiology, 1997. **63**(7): p. 2759-2764.
61. DeAngelis, P.L., *Hyaluronan synthases: fascinating glycosyltransferases from vertebrates, bacterial pathogens, and algal viruses.* Cell Mol Life Sci, 1999. **56**(7-8): p. 670-82.

APPENDIX A: Supplemental Figures

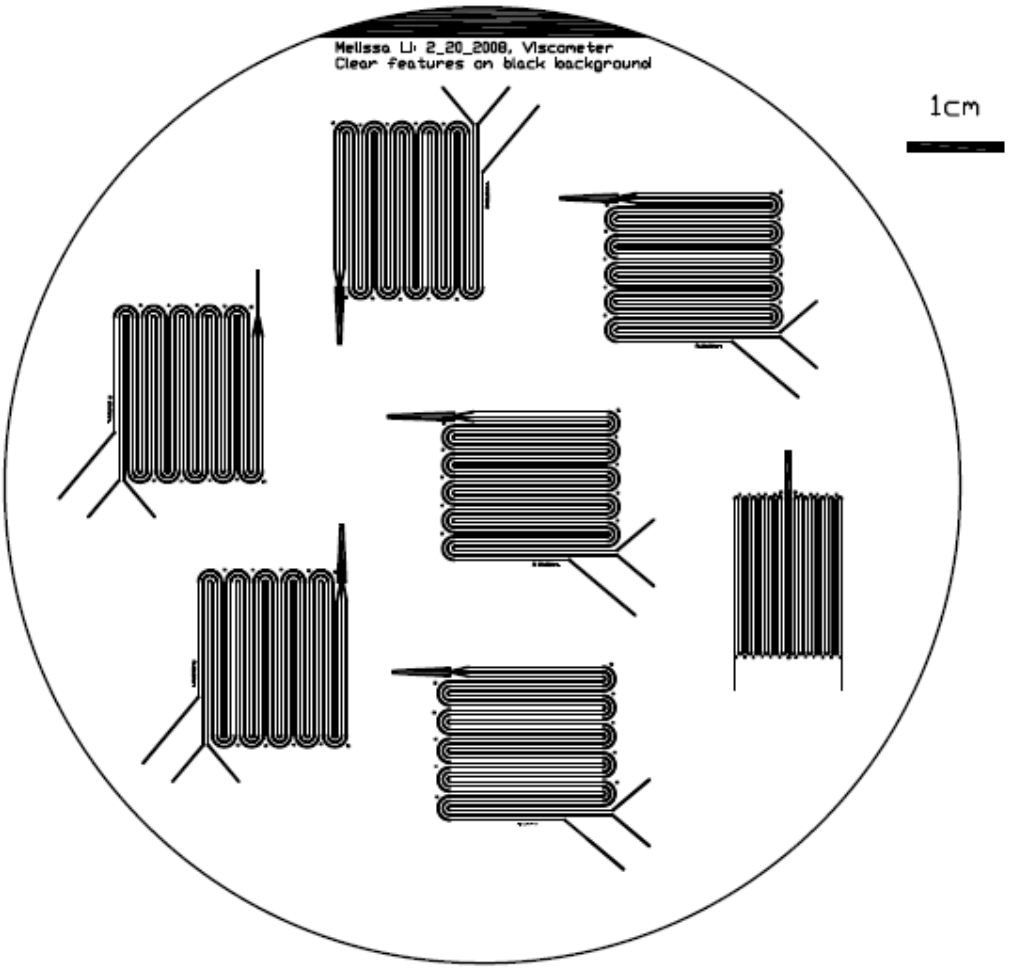

Figure A: *Viscometer device photo-mask*

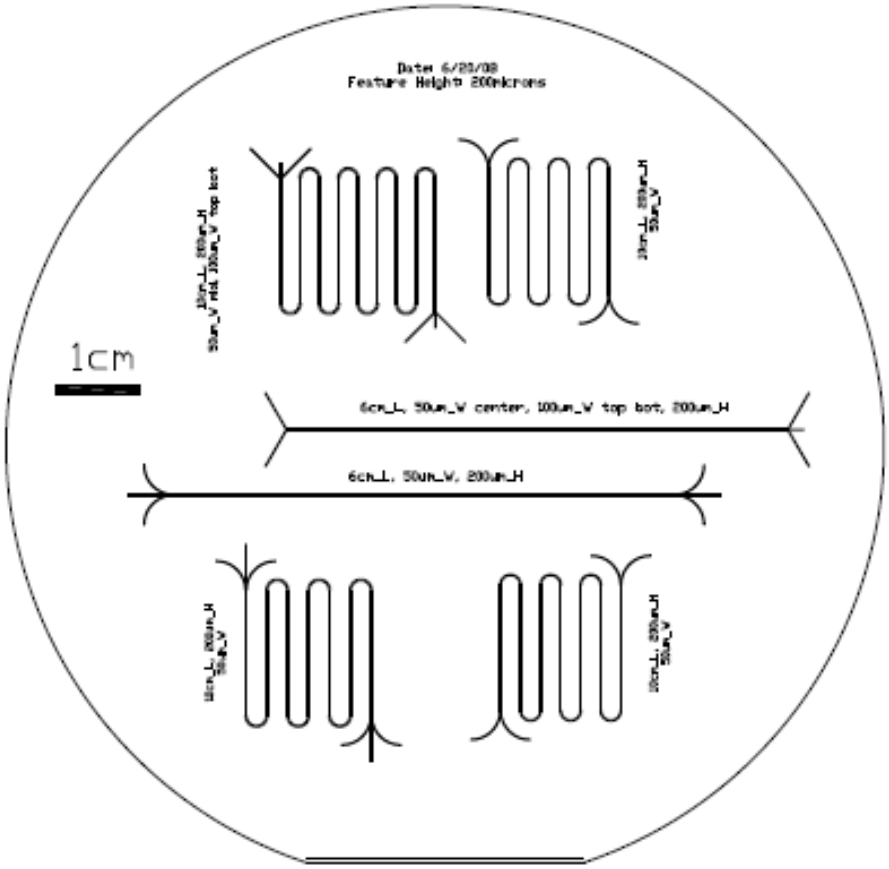

Figure B: *Dialysis device photo-mask*

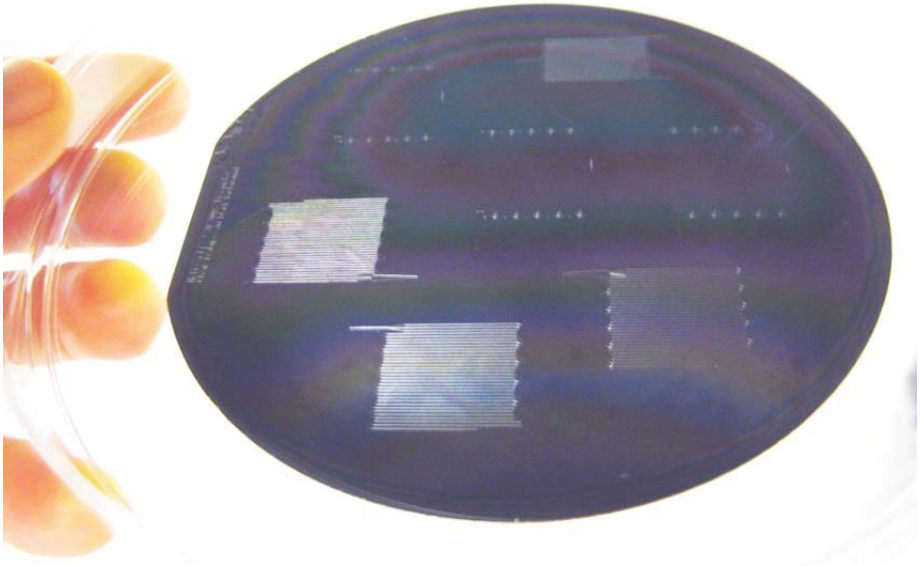

Figure C: *A silicon wafer patterned with SU8 photodeveloper features using UV light*

```
clear all;
close all;

user_info = input('\n Which movie would you like to analyze? \n', 's');

z=trackprog7(user_info);
visc_data=stream_label10(user_info);
```

```
function z=trackprog7(user_info,thres)

%% read in movie file
thres = 1/6;
start_mov=7;
%x=aviread(user_info,start_mov:end_mov); %file feed
x=aviread(user_info);
info=aviinfo(user_info);
end_mov=info.NumFrames;
%end_mov=100;
save info info; %save info about movie for stream_label
%num=end_mov-start_mov+1; %frames of movie
warning off;
%%  filter original movie
bg_frame = start_mov; %this frame will be subtracted background

for i=start_mov:end_mov
    p1(:,:,i)=imresize(x(i).cdata(:,:,2),.8); %put 0-256 from struct
about num_frames into p1
end

num = size(p1,3); %num is the number of frames of the movie
for i=1:num
    p1(:,:,i)=medfilt2(medfilt2(medfilt2(p1(:,:,i)))); %median filter
three times each frames
end

background = p1(:,:,bg_frame);
save background background;

for i=1:num
      pdiff(:,:,i)=imsubtract(p1(:,:,i),background);
end

clear p1;

%% BW transformation
m=max(max(max(pdiff(:,:,1:num))));
```

```
% THRESHOLD YOUR MOVIE
for i=1:num %range from 1/3 (high thres) to 1/7 (low thres)
    p_bw(:,:,i)=im2bw(pdiff(:,:,i),double(m)/256*thres); %im2bw
replaces all pixels in p_diff>(max/256*1/5) with white
end

clear pdiff

for i=1:num
    p_filt4(:,:,i)=bwareaopen(p_bw(:,:,i),70,4); %filter all spots
<20px
end

%% various filters...

figure(); imshow(p_filt4(:,:,size(p_filt4,3)));
p_filt4 = imresize(p_filt4,.625);
p_filt4 = uint8(p_filt4);

save bw_movie p_filt4;
save thres;
clear all;
z=1;
```

```
function  visc_data=stream_label10(user_info)


%% Add start length data
L1=1.7; %%mm of start length offscreen
L2=2;
L3=7.728; %%L3 should be last stream to come onscreen

%% Label areas
load bw_movie.mat;
last_bw=p_filt4(:,:,size(p_filt4,3));
[p_bwlbl,objs]=bwlabeln(p_filt4);
clear p_filt4;
p_bwlbl = uint8(p_bwlbl);
%label the filtered bw matrix by contiguous block
% for i=1:size(p_bwlbl,3)
%   imshow(label2rgb(p_bwlbl(:,:,i),@jet))
%    pause(.1)
% end
%% Calculate pixels in stream per frame

p_bwlbl2(:,:,1)=p_bwlbl(:,:,1);

%conserve pixel noise
for i=2:size(p_bwlbl,3) %for whole movie from second frame on...
    x = zeros(size(p_bwlbl(:,:,i))); %start with blank image
    for j=1:3 %examine by obj...only want to append to largest 3
    locs = find(p_bwlbl(:,:,i)==j); %find this obj in this frame
    locs_prev = find(p_bwlbl2(:,:,i-1)==j); %...and in previous frame
```

```
    locs = cat(1,locs,locs_prev); %combine locations
    x(locs)=j; %label locations of obj in this frame and prev
    p_bwlbl2(:,:,i) = x; %add these map locations
    end
end
clear x;
save p_bwlbl; %save label movie to file
clear p_bwlbl;
p_bwlbl2=uint8(p_bwlbl2);
figure();
last_label=p_bwlbl2(:,:,size(p_bwlbl2,3));
imshow(label2rgb(p_bwlbl2(:,:,size(p_bwlbl2,3)),@jet));

%% Get length and velocity data
%create matrix of total area of object (total #pixels) in frame
for i=1:size(p_bwlbl2,3)
    for j=1:objs
    [r,c]= find(p_bwlbl2(:,:,i)==j);
    obj_pixels(i,j)= length(r); %matrix: rows = frame, col = obj
    end
end
obj_pixels=double(obj_pixels);
pix_to_mm = max(obj_pixels(size(obj_pixels,1),:))/189; %pixel
conversion should be max amt of pixel length / theoretical
%pix_to_mm = 117;
obj_length=obj_pixels/pix_to_mm;
obj_length(:,1)=L1+obj_length(:,1); %add initial off-chip lengths
obj_length(:,2)=L2+obj_length(:,2);
obj_length(:,3)=L3+obj_length(:,3);

%% Calculate velocity and lt_vt using Han II
%create matrix for difference in area over frame
nframes = 2; %choose num frames to take speed over
t=1:1:size(obj_pixels,1);
load info.mat %load movie info file
fps = info.FramesPerSecond;
t=t/fps; %time is in seconds
clear info.mat;

for i=(nframes+1):size(p_bwlbl2,3)-nframes
    for j=1:objs
    obj_vel(i,j)= (obj_length(i,j)-obj_length(i-
nframes,j))/((nframes)/fps);
    lt_vt2(i,j)=((obj_length(i,j))^2-(obj_length(i-
nframes,j))^2)/((nframes)/fps);
    end
end
%pad matrices with zeros)
pad_ins=zeros(nframes, objs);
obj_vel = cat(1,pad_ins,obj_vel);
lt_vt2=cat(1, pad_ins, lt_vt2);

lt_vt1=obj_length.*obj_vel; %lt_vt Han Method I

%% Post-processing/Clean up data:
% Use only matrix with points lt_vt2>0 and <lt_vt2_thres
```

```
a = lt_vt2(:,1); %a is a matrix of only columns 1-3
for (i=2:3)
    j = lt_vt2(:,i);
    a = horzcat(a,j);
end

%Create new
%1.  lt_vt2_band matrix of values>0 and <thres maximum value
lt_vt2_thres = 3000; %maximum lt_vt2 value
[r1,c1]=find(a>0&a<lt_vt2_thres); %return locations of the found terms
where r is row, c is column)
[r2,c2]=find(a==0|a>lt_vt2_thres);%return locations of the found terms
where r is row, c is column)
b1=unique(r1); %condense find results in r1 to a sorted array of row
indices
b2 = unique(r2);
index_lt_vt2_band = setdiff(b1,b2);
lt_vt2_band = lt_vt2(index_lt_vt2_band,:);
lt_vt2 = lt_vt2_band;

%2.  new t_vect_band to give times
t_vect = index_lt_vt2_band/fps; %create new time vector which retains
the real times
t= t_vect;

%% return data back to managing function
load info.mat info;
load thres thres;

visc_data = struct('length_pix', obj_pixels,'length_mm', obj_length,
'vel_mm_s', obj_vel,'lt_vt1',lt_vt1,'lt_vt2', lt_vt2, 'info', info,
'thres', thres, 't',transpose(t),'label', last_label,'bw', last_bw);
save visc_data; %1st time saves for calc_stats function
disp('Sample Viscosities:');
stats = calc_stats();
filetag=strcat('v_',user_info);
visc_data = struct('length_pix', obj_pixels,'length_mm', obj_length,
'vel_mm_s', obj_vel,'lt_vt1',lt_vt1,'lt_vt2',
lt_vt2,'info',info,'thres',thres,'t',transpose(t),'label',last_label,'b
w',last_bw,'stats',stats,'lt_vt2_thres',lt_vt2_thres,'p_bwlbl2',
p_bwlbl2);
save (filetag,'visc_data'); %second time saves for reference
save p_bwlbl2 p_bwlbl2;

load p_bwlbl2;
%%
figure(3);
for i=1:size(p_bwlbl2,3)
    imshow(label2rgb(p_bwlbl2(:,:,i)));
    pause (.1);
end
```

```
 function stats = calc_stats()

%% Plot the Lt_vt data Han style
```

```
load visc_data;

std_lt_vt2=std(visc_data.lt_vt2,0,1); %standard deviation of each
lt_vt2 object
t = visc_data.t;

for i=1:3 %for each of the 3 objects
    [p3,S3]=polyfit(visc_data.lt_vt2(:,3),visc_data.lt_vt2(:,i),1);
%plot sample vs reference
        visc(i,3)=p3(1); %linear coefficient
        P=visc_data.lt_vt2(:,i); Pp =
polyval(p3,visc_data.lt_vt2(:,3)); %expected Pp vs exptl P
        d=P-Pp;
        r2_3=1-sum(d.^2)/sum((P-mean(P)).^2); %calculate the R^2 value
for this set
    [p2,S2]=polyfit(visc_data.lt_vt2(:,2),visc_data.lt_vt2(:,i),1);
        visc(i,2)=p2(1);
        P=visc_data.lt_vt2(:,i); Pp =
polyval(p2,visc_data.lt_vt2(:,2));
        d=P-Pp;
        r2_2=1-sum(d.^2)/sum((P-mean(P)).^2);
    [p1,S1]=polyfit(visc_data.lt_vt2(:,1),visc_data.lt_vt2(:,i),1);
        visc(i,1)=p1(1);
        P=visc_data.lt_vt2(:,i); Pp =
polyval(p1,visc_data.lt_vt2(:,1));
        d=P-Pp;
        r2_1=1-sum(d.^2)/sum((P-mean(P)).^2);

    p = cat(1,p1,p2,p3);
    S = cat(1,S1,S2,S3);
    r2 = cat(1,r2_1,r2_2,r2_3); %matrix of all r^2 values for this
object

     p_lt_vt2(:,:,i)=p;
     S_lt_vt2(:,i)=S;
     r2_lt_vt2(:,i)=r2;%column 1 is all R^2 values for object vs 1,2,3
end

S = struct('S',S_lt_vt2);
p = struct('p', p_lt_vt2);

stats = struct('r2', r2_lt_vt2, 'S', S, 'p',p, 'visc', visc);
fprintf('Viscosity using middle lane as reference:');
fprintf('/n');
matshow = cat(2,visc(:,1),r2_lt_vt2(:,1));
matshow
```